

University of Dundee

Mild stress conditions during laboratory culture promote the proliferation of mutations that negatively affect Sigma B activity in *Listeria monocytogenes*

Guerreiro, Duarte N.; Wu, Jialun; Dessaux, Charlotte; Oliveira, Ana H.; Tiensuu, Teresa; Gudynaite, Diana

Published in:
Journal of Bacteriology

DOI:
[10.1128/JB.00751-19](https://doi.org/10.1128/JB.00751-19)

Publication date:
2020

Document Version
Peer reviewed version

[Link to publication in Discovery Research Portal](#)

Citation for published version (APA):

Guerreiro, D. N., Wu, J., Dessaux, C., Oliveira, A. H., Tiensuu, T., Gudynaite, D., Marinho, C. M., Boyd, A., García-Del Portillo, F., Johansson, J., & O'Byrne, C. P. (2020). Mild stress conditions during laboratory culture promote the proliferation of mutations that negatively affect Sigma B activity in *Listeria monocytogenes*. *Journal of Bacteriology*, 202(9), [e00751-19]. <https://doi.org/10.1128/JB.00751-19>

General rights

Copyright and moral rights for the publications made accessible in Discovery Research Portal are retained by the authors and/or other copyright owners and it is a condition of accessing publications that users recognise and abide by the legal requirements associated with these rights.

- Users may download and print one copy of any publication from Discovery Research Portal for the purpose of private study or research.
- You may not further distribute the material or use it for any profit-making activity or commercial gain.
- You may freely distribute the URL identifying the publication in the public portal.

Take down policy

If you believe that this document breaches copyright please contact us providing details, and we will remove access to the work immediately and investigate your claim.

1 **Mild stress conditions during laboratory culture promote the proliferation of**
 2 **mutations that negatively affect Sigma B activity in *Listeria monocytogenes***

3
 4
 5 Duarte N. Guerreiro^a, Jialun Wu^a, Charlotte Dessaux^b, Ana H. Oliveira^c, Teresa
 6 Tiensuu^c, Diana Gudynaite^d, Catarina M. Marinho^{a,e,f}, Aoife Boyd^g, Francisco García-del
 7 Portillo^b, Jörgen Johansson^c, Conor P. O'Byrne^{a#}

8
 9
 10 ^aBacterial Stress Response Group, Microbiology, School of Natural Sciences, National
 11 University of Ireland Galway, H91 TK33, Ireland

12 ^bLaboratory of Intracellular Bacterial Pathogens, National Center for Biotechnology
 13 (CNB)-CSIC, Madrid-Spain

14 ^cLaboratory for Molecular Infection Medicine Sweden, Department of Molecular Biology,
 15 Umeå Centre of Microbial Research, Umeå, Sweden

16 ^dMolecular Microbiology Department, School of Life Sciences, University of Dundee

17 ^eUniversité de Bourgogne Franche-Comté, Dijon, France

18 ^fInstitut National de la Recherche Agronomique, UMR Agroécologie, Dijon, France

19 ^gPathogenic Mechanisms Research Group, National University of Ireland Galway,
 20 Ireland

21
 22
 23 Running title: *sigB* operon mutations increase growth under stress

24
 25
 26 #Address correspondence to Conor O'Byrne, conor.obyrne@nuigalway.ie
 27

28 **Abstract**

29 In *Listeria monocytogenes* the full details of how stress signals are integrated into the σ^B
30 regulatory pathway are not yet available. To help shed light on this question we
31 investigated a collection of transposon mutants that were predicted to have
32 compromised activity of the alternative sigma factor B (σ^B). These mutants were tested
33 for acid tolerance, a trait that is known to be under σ^B regulation, and they were found to
34 display increased acid sensitivity, similar to a mutant lacking σ^B ($\Delta sigB$). The transposon
35 insertions were confirmed by whole genome sequencing, but in each case the strains
36 were also found to carry a frameshift mutation in the *sigB* operon. The changes were
37 predicted to result in premature stop codons, with negative consequences for σ^B
38 activation, independently of the transposon location. Reduced σ^B activation in these
39 mutants was confirmed. Growth measurements under conditions similar to those used
40 during the construction of the transposon library revealed that the frameshifted *sigB*
41 operon alleles conferred a growth advantage at higher temperatures, during late
42 exponential phase. Mixed culture experiments at 42°C demonstrated that loss of σ^B
43 activity allowed mutants to take-over a population of parental bacteria. Together, our
44 results suggest that mutations affecting σ^B activity can arise during laboratory culture
45 because of the growth advantage conferred by these mutations under mild stress
46 conditions. The data highlight the significant cost of stress protection in this food-borne
47 pathogen and emphasise the need for whole genome sequence analysis of newly
48 constructed strains to confirm the expected genotype.

51 **Importance**

52 In the present study we investigated a collection of *Listeria monocytogenes* strains that
53 all carried *sigB* operon mutations. The mutants all had reduced σ^B activity and were
54 found to have a growth advantage under conditions of mild heat stress (42°C). In mixed
55 cultures these mutants outcompeted the wildtype when mild heat stress was present but
56 not at an optimal growth temperature. An analysis of 22,340 published *L.*
57 *monocytogenes* genome sequences found a high rate of premature stop codons
58 present in genes positively regulating σ^B activity. Together the findings suggest that the

occurrence of mutations that attenuate σ^B activity can be favoured under conditions of mild stress, probably highlighting the burden on cellular resources that stems from deploying the general stress response.

Introduction

Listeria monocytogenes is the causative agent of listeriosis, which can sicken immunocompromised individuals and pregnant women and is associated with a high mortality rate (typically 25-30%) (1, 2). *L. monocytogenes* is ubiquitous in the environment (3) partly due to its ability to survive and grow in a wide range of harsh conditions, such as low pH, high osmolality (4) and elevated concentrations of bile salts (5). This robustness is partly under the control of the stress-inducible sigma factor sigma B (σ^B), which is responsible for the upregulation of a regulon composed of approximately 300 genes (6, 7). σ^B also plays a role in establishing infections, as it is necessary for *L. monocytogenes* survival in the gastrointestinal tract (8) and it contributes to the regulation of the internalin genes *inlA* and *inlB* that are required for host cell invasion (9).

In *Bacillus subtilis*, σ^B is regulated by a signal transduction pathway that is primarily encoded in the polycistronic *sigB* operon, which comprises eight genes, *rsbR*, *rsbS*, *rsbT*, *rsbU*, *rsbV*, *rsbW*, *sigB* and *rsbX* (10). In *L. monocytogenes* two additional genes, *mazE* and *mazF*, are located upstream of *rsbR* are also co-transcribed with this operon (11). The σ^B signal transduction pathway has been well studied in *B. subtilis*, where the main components of the system are all conserved and share a high degree of similarity with their *L. monocytogenes* counterparts (12). In the absence of stress the anti-sigma factor RsbW sequesters σ^B , blocking its interaction with RNA polymerase (13, 14). Upon encountering environmental or starvation stress an unknown signal is detected and integrated by the stressosome, a supramolecular complex composed of RsbR, RsbS and RsbT (15-18), as well as a number of RsbR paralogues (Lmo0161, Lmo0799, Lmo1642 and Lmo1842) (19, 20). This triggers the serine-threonine kinase activity of

RsbT, resulting in the phosphorylation of RsbR and RsbS and subsequent release of RsbT from the stressosome (21, 22). Once free, RsbT interacts with RsbU activating its serine phosphatase activity, which in turn results in the dephosphorylation of the anti-anti-sigma factor RsbV. The anti-sigma factor RsbW, which is also a serine kinase, possesses a higher affinity with the non-phosphorylated RsbV than σ^B , resulting in the sequestration of RsbW by RsbV and the release σ^B (23), allowing it to interact with RNA polymerase and instigate transcription of the σ^B regulon.

Several studies, both in *L. monocytogenes* and *B. subtilis*, have shown that mutations constructed within the *sigB* operon result in reduced σ^B activity as a consequence of impaired signal transduction through this pathway (21, 24-28). Although the main elements of the signal transduction pathway from the stressosome to σ^B is well described, the nature of the signals detected and the molecular mechanisms involved in the transduction of these signals are still largely unknown. Paradoxically a number of studies have reported that loss of *sigB* can result in a faster growth rate under some culture conditions. In a chemically defined medium with limiting glucose mutant strains lacking either *sigB*, *rsbV* or *rsbT* grow faster at 37°C than the WT (29). At 3°C a growth advantage has also been reported for a *sigB* mutant strain in complex medium (30). In the presence of sub-lethal doses of blue light, mutant strains lacking σ^B show improved growth in both liquid and solid complex media (31). These findings suggest that deploying the σ^B -controlled general stress response can under some conditions impose a cost on cells that results in a reduced growth rate.

In an attempt to develop a better understanding of the factors that influence stress sensing via the stressosome we focussed on a set of transposon mutant strains in *L. monocytogenes* EGD-e that were previously suggested to have altered σ^B activity (32). In their study, Tiensuu and colleagues discovered that *L. monocytogenes* forms distinct rings in soft agar plates when exposed to cycles of light and darkness, a phenotype that is mediated by σ^B and requires the action of RsbL (also known as Lmo0799), a

121 stressosome-associated RsbR paralogue that acts as a blue-light sensor (19). The
122 authors described the isolation of several transposon mutant strains that failed to
123 produce these rings in response to oscillating cycles of light ("ringless" phenotype) and
124 suggested that the genes carrying the transposon insertions could be involved in
125 modulating σ^B activity. The present study focussed on this collection on mutant strains
126 in the expectation that the mutated genes might give new insights into the mechanisms
127 that lead to the activation of σ^B in response to stress and potentially into the nature of
128 the stress signals detected.

129

130

131 During the preliminary stages of the present study whole genome sequencing (WGS)
132 was used to confirm the location of the transposon insertions. While confirming the
133 presence of the transposons it also revealed the presence of distinct frameshift
134 mutations in the *sigB* operon in each of the ringless strains. This suggested a simpler
135 explanation for the ringless phenotype of the transposon mutant strains; namely that the
136 *sigB* operon alleles reduced σ^B activity which in turn compromised the "ring" formation.
137 The emergence of mutations in the *sigB* operon of *L. monocytogenes* during laboratory
138 culture has been reported in a number of other studies (28, 31, 33-35). It has been
139 suggested that the occurrence of mutations impairing σ^B function might be particularly
140 associated with loss of surface proteins (36). However, the selective pressure driving
141 the emergence of these alleles is unknown. Here, we investigated the properties of
142 these *sigB* operon mutant strains to determine whether σ^B activity was affected and
143 whether that affected their fitness. The frameshift alleles that arose in the *sigB* operon of
144 these strains were associated with reduced acid tolerance, as well as a marked
145 reduction in σ^B activity. Furthermore, in the presence of mild heat stress the mutations
146 produced a fitness advantage in mixed populations with WT bacteria that was
147 qualitatively similar to that seen in a *sigB* deletion mutant strain. Together, these
148 observations suggest that loss of σ^B activity can confer a growth advantage under
149 conditions used routinely during laboratory culture of *L. monocytogenes*. We propose
150 that this effect is responsible for the common emergence of mutations in the *sigB*

operon under laboratory conditions, and that this finding has important implications for researchers studying any phenotypic properties of this pathogen.

Results

“Ringless” transposon mutants display acid-sensitive phenotypes.

Five “ringless” transposon mutant strains from the study of Tiensuu *et al.* (A4:E8, C10:A8, C14:C12, D9:B6 and D2:C10 (32). Herein renamed as 1RsbS (H23R), 2RsbU (E103K), 3RsbS (H23R), 4RsbV (E42R), 5RsbV (R47Y), respectively) were selected to investigate the possible effects of these insertions on the regulation of σ^B activity in *L. monocytogenes* EGD-e (Table 1 and 2). These “ringless” mutant strains were first reconfirmed to be defective for ring formation (data not shown), a phenotype exhibited on soft agar media in response to 12 hour cycles of light and dark and known to be under σ^B control (32) (Table 1). Since σ^B plays an important role in acid tolerance we reasoned that transposon mutations influencing σ^B activity would also lead to an altered acid resistance phenotype. To investigate this the 5 “ringless” mutant strains were tested for their ability to withstand a challenge at pH 2.5 and compared to the WT (EGD-e) and two control strains that harbour a transposon insertion but still retained the “ring” phenotype (B14:A6 and B15:E2) (32). The WT and the 2 ring-forming strains behaved similarly in this assay, showing high resistance to lethal acidic conditions, while a mutant strain lacking σ^B ($\Delta sigB$) was exquisitely sensitive to acid, showing significantly decreased viable counts at 30 min and no viable counts at 60 min (Fig. 1). The “ringless” transposon mutant strains all displayed a significant increase in acid sensitivity compared to the ring-forming WT and ring-forming control strains. These data strongly suggested that σ^B activity was compromised in these strains.

The “ringless” transposon mutants harbour secondary mutations in the *sigB* operon conferring a reduced σ^B activity.

To assess whether additional mutations could be present in the transposon mutant strains displaying the ring and “ringless” phenotype, we performed WGS on each of

182 them. The location of the transposon insertions was found to be identical to those
 183 described by Tiensuu *et al.* (32) for eight of the strains tested (Table 2). However there
 184 were three exceptions; the *loci* reported to carry the transposon insertions in strains
 185 1RsbS (H23R) (*Imo0040*), 2RsbU (E103K) (*Imo0124*) and 4RsbV (E42R) (*Imo0101*)
 186 were somewhat different in the WGS analysis that we performed (Table 2). This
 187 difference is likely due to the different methods used to determinate their position in the
 188 two studies.

189
 190
 191 An analysis of the genome sequences for single nucleotide polymorphisms (SNPs)
 192 revealed that all eleven of the “ringless” mutant strains had mutations in the *sigB*
 193 operon. Specifically, either the *rsbS*, *rsbU* or *rsbV* genes carried frameshift mutations
 194 that were predicted to result in deeply truncated versions of the corresponding protein
 195 products (Fig. 2 and Table 2). Six of the transposon mutant strains carried the same
 196 mutant allele in the *rsbS* gene, a four nucleotide insertion resulting in a premature stop
 197 at codon 38 (H23R; Table 2). The other five mutant strains all carried unique frameshift
 198 alleles in *rsbU*, *rsbS*, or *rsbV* (Table 2). The two ring-forming control strains selected for
 199 our study (B14:A6 and B15:E2) showed no mutation in any of the *sigB* operon genes.
 200 Based on the known functions of the proteins encoded by the *sigB* operon it seemed
 201 likely that these mutations, rather than the transposon insertions, were responsible for
 202 both the “ringless” and acid-sensitive phenotypes.

203
 204
 205 To investigate this further we focused attention on strain 3RsbS (H23R), predicted to
 206 express a truncated RsbS protein, since the loss of ring formation in this transposon-
 207 carrying strain was partially complemented in the study by Tiensuu *et al.* by providing
 208 the gene affected by the transposon insertion (*Imo0596*) *in trans* (32). The
 209 complementation suggested that the transposon insertion was responsible for the
 210 ringless phenotype, rather than the SNP in the *rsbS* gene, which we now suspected to
 211 be the principal cause of the phenotype. The WGS analysis revealed that the
 212 transposon was located 186 bp upstream from the start codon of *Imo0596* and 40

213 upstream from the divergently transcribed gene *sreB*, which encodes a sRNA S-
214 adenosylmethionine (SAM) riboswitch (37). We reasoned that if disruption of either
215 *lmo0596* or *sreB* was responsible for the ringless phenotype then deletion of either gene
216 should produce a similar phenotype. Deletion of neither gene produced a ringless
217 phenotype, whereas loss of *sigB* produced the expected loss of ring formation (Fig. S1
218 A). If the transposon impacted σ^B activity through effects on either *lmo0596* or *sreB* then
219 loss of these genes might be expected to affect acid tolerance, another highly σ^B -
220 dependent phenotype. However deletion of neither gene produced any detectable effect
221 on survival at pH 2.5, unlike the $\Delta sigB$ mutation, which produced an acid sensitive
222 phenotype (Fig. S1 B & C). Similarly, if the transposon insertion in this strain was
223 affecting σ^B activity via an effect on these genes the transposon might be expected to
224 affect the transcription of one or both genes. RT-qPCR was used to measure the
225 relative levels of *lmo0596* and *sreB* transcription in the transposon carrying strain
226 3RsbS compared to the wild-type, the $\Delta sigB$ mutant, and two other transposon-carrying
227 strains (the ring forming strain B12:A6 and the ringless strain 1RsbS). The transcription
228 of *lmo0596* was confirmed to be σ^B -dependent, as earlier suggested (38), but no
229 difference in transcription was observed between the 3RsbS and 1RsbS strains, which
230 carry transposon insertions in completely separate *loci* (Fig. S1 D; Table 2). Neither was
231 *sreB* transcription affected by the presence of the transposon (Fig. S1 D). Finally, the
232 deletion of *lmo0596* had no effect on the transcription of the σ^B -dependent gene
233 *lmo2230* suggesting that this gene does not play a role in regulating σ^B activity (Fig. S1
234 E). Taken together these results suggest that the transposon insertion in strain 3RsbS is
235 not responsible for the observed ringless phenotype in 3RsbS (H23S) and we therefore
236 we conclude that the altered phenotype in the 3RsbS (H23R) transposon mutant is
237 solely due to the frameshift mutation in *rsbS*, and suggest that the *sigB* operon
238 mutations in the other strains are most likely responsible for their σ^B -related phenotypes
239 too.

240
241
242 To investigate this further σ^B activity was measured in these strains using a previously
243 described transcriptional reporter that fuses the highly σ^B -dependent promoter of

244 *lmo2230* (annotated as a putative arsenate reductase) to the enhanced green
245 fluorescent protein gene (*egfp*) (39). This reporter was integrated into the genome,
246 upstream of the original promoter of *lmo2230*, of the WT, the $\Delta sigB$ mutant strain and
247 seven of the transposon insertion strains, including five “ringless” and two ring-forming
248 control strains. Fluorescence was recorded by fluorescence microscopy following
249 growth to stationary phase at 37°C, a condition where σ^B is known to be highly active
250 (24, 39). As expected the $\Delta sigB$ mutant strain had almost no detectable fluorescence
251 while the WT and ring-forming transposon control strains (B14:A6 and B15:E2)
252 produced a strong fluorescent signal (Fig. 3 A & B). In contrast the “ringless” strains that
253 carried mutations in *rsbS*, *rsbU* or *rsbV* all produced a greatly reduced fluorescence
254 signal, albeit not as low as the $\Delta sigB$ deletion mutant strain. Western-blotting was used
255 to determine the levels of eGFP protein in the reporter strains under the same growth
256 conditions. The results confirmed what was observed microscopically; very low levels of
257 eGFP expression in the $\Delta sigB$ mutant strain and in the strains harbouring *sigB* operon
258 mutations, but not in the WT or ring-forming transposon mutant strains (Fig. 3 C & D).
259 These data confirmed that σ^B activity was reduced in the strains that displayed both an
260 acid-sensitive and ringless phenotype. The most parsimonious explanation for these
261 observations is that the *sigB* operon alleles in the “ringless” mutant strains were directly
262 responsible for the reduced σ^B activity and associated phenotypes, especially since
263 defined mutations in these genes, in both *L. monocytogenes* and *B. subtilis*, have
264 previously been shown to result in reduced σ^B activity (14, 27-29, 31, 36, 40, 41).
265 Moreover, the ring-forming transposon mutant strains used as controls exhibited similar
266 phenotypes to the WT strain. It is highly unlikely therefore that the transposons
267 themselves were responsible for any of the phenotypes detected in these strains.

268

269

270 **The *rsbS* frameshift results in a polar effect on *rsbT*.**

271 The *sigB* operon has the gene order *mazEF-rsbRSTUVW-sigB-rsbX*, with a σ^A promoter
272 located upstream from *rsbR* and a σ^B -dependent promoter upstream from *rsbV* (Fig. 2).
273 Mutations in *rsbS*, *rsbU* and *rsbV* could potentially produce polar effects on downstream
274 genes further impacting the pathway leading to σ^B activation. To address this western-

275 blots were performed using polyclonal antibodies against RsbT and σ^B on each of the
276 strains. The levels of RsbT were markedly reduced in the “ringless” strains carrying the
277 *rsbS* H23R allele but were similar to the WT in the strains carrying either the *rsbU* or
278 *rsbV* frameshift alleles (Fig. 4 A). In contrast the levels of σ^B protein were similar in all
279 the strains (with the exception of the $\Delta sigB$ mutant strain) (Fig. 4 B). These data show
280 that the effects of the *rsbU* and *rsbV* frameshift alleles on σ^B activity are probably
281 directly caused by the loss of these proteins. The *rsbS* frameshift allele affects the
282 expression of RsbT, suggesting that these genes may be translationally coupled and
283 that the loss of σ^B activity in this strain likely arises through a loss of both stressosome-
284 associated proteins.

285

286

287 **Reduced σ^B activity confers increased growth rate at higher temperatures.**

288 Since the procedure for generating the transposon mutants involved an incubation step
289 at a range of different temperatures (32, 42) we hypothesised that *sigB* operon
290 mutations might arise if the mutant strains had a growth advantage in these conditions.
291 To assess this cultures of the WT, $\Delta sigB$ mutant strain, one of the “ringless” mutant
292 strain (designated 2RsbU (E103K)) and a ring-forming transposon mutant strain control
293 (B14:A6) were grown at 30°C, 37°C, 40°C and 42°C and their growth rates determined
294 (Fig. 5). At 30°C there was no significant effect of the genotype on the growth rates,
295 whereas at the higher temperatures the “ringless” mutant strains lacking *sigB* or with an
296 *rsbU* frameshift allele (E103K) exhibited a slight increase in the growth rate. At 42°C
297 these two mutant strains grew noticeably faster than the WT and ring-forming control
298 B14:A6 strains, especially as the cultures approached stationary phase between 4 to 7
299 h after inoculation (Fig. 5 D). This finding raised the possibility that mutations arising
300 spontaneously in the *sigB* operon could be selected for at higher temperatures because
301 of a growth advantage relative to WT cells possibly due to the reduced σ^B activity.

302

303

304 To further examine this possibility we performed mixed culture competition experiments
305 to determine if the growth rate advantage would enable the $\Delta sigB$ and *sigB* mutants to

306 outcompete the WT during growth at elevated temperatures. Cultures were prepared
307 that mixed the WT with the $\Delta sigB$ mutant strain or the “ringless” *rsbU* mutant strain
308 (2RsbU (E103K)) or the ring-forming control strain B14:A6 mutant strain in a ratio of
309 1000:1 (WT:mutant). Cultures were grown over a period of 5 days, with a daily passage
310 into fresh medium and dilutions were plated daily onto BHI agar to determine the
311 relative proportion of each strain. The erythromycin resistance of the transposon
312 containing strains was used to differentiate the WT from mutant strains, while a
313 difference in the colony colour was used to discriminate the WT and the $\Delta sigB$ mutant
314 strain, as described in the materials and methods. When the mixed cultures were grown
315 at 42°C the “ringless” mutant strains carrying the *rsbU* frameshift allele accumulated
316 steadily, reaching approximately 50% of the population after 5 days (Fig. 6 A). In
317 contrast the ring-forming control strain did not accumulate in the culture over this period
318 (Fig. 6 B). At 42°C the $\Delta sigB$ mutant strain accumulated within the population,
319 dominating it (80:20) by the end of 5 days. However at 30°C, where this growth
320 advantage was absent (Fig. 5 A), the $\Delta sigB$ mutant strain failed to fully dominate the
321 population, reaching approximately 10% by the end of 5 days (Fig. 6 D). When cultures
322 were mixed 1:1 and grown at 42°C the advantage was less evident for the “ringless”
323 strain carrying the *rsbU* allele but the $\Delta sigB$ mutant strain still dominated the WT under
324 these conditions (Fig. S2). When the WT was started as the minority strain (1:1000) in
325 these competition assays it failed to emerge as the dominant population when
326 competed against any of three mutant strains tested (Fig. S2 E-G). Overall the data
327 suggest that strains with reduced σ^B activity can accumulate in a mixed population when
328 the growth temperature is elevated.

329

330

331 **Loss of *rsbX* results in reduced competitiveness.**

332 The observations above suggest that a growth advantage arises in strains with reduced
333 σ^B activity when a mild heat stress is present. A corollary of this conclusion is that
334 increased σ^B activity might be expected have a negative effect on growth and
335 competitiveness. In the current model of σ^B regulation in *L. monocytogenes* RsbX is
336 believed to act as phosphatase whose function is to reset the resting state of the

337 stressosome following a stress signalling event (43, 44). Thus RsbX plays a negative
 338 role in regulating σ^B activity and the loss of RsbX is expected to have produced a strain
 339 with elevated σ^B activity. To investigate this, competition experiments were performed
 340 with a $\Delta rsbX$ mutant strain to test the competitiveness of this strain relative to the WT at
 341 both 30°C and 42°C (Fig. 7). When $\Delta rsbX$ was present as the minority strain (1000-fold
 342 under-represented at the start of the experiment) it failed to dominate the culture over 5
 343 days of passaging, regardless of the temperature (Fig. 7 A & B), although it did recover
 344 its population somewhat over this period. When the WT was the minority strain it
 345 outgrew $\Delta rsbX$ over the same time period (Fig. 7 C & F), showing that the WT had a
 346 competitive advantage over the mutant strain. When the populations were equal at the
 347 start of the experiment the WT tended to dominate the mixed cultures (Fig. 7 B & E).
 348 This result was observed at both incubation temperatures, probably because the growth
 349 of the $\Delta rsbX$ strain was inhibited regardless of the temperature. Overall these results
 350 are consistent with the idea that mutations that increase σ^B activity produce a growth
 351 disadvantage.

352
 353
 354 **Premature stop codons occur with a higher than average frequency in the**
 355 **positive regulators of σ^B within the *sigB* operon.**

356 The occurrence of *sigB* operon mutations in this study and in other studies (28, 31, 33-
 357 36) prompted us to investigate whether undocumented premature stop codons
 358 (PMSCs) might be present in the *sigB* operon in genome sequences deposited in public
 359 databases, so we searched for PMSCs in the *sigB* operon among 22,340 of *L.*
 360 *monocytogenes* genome assemblies. The PMSC rate per 100 bp (expressed as a %
 361 rate per 100 bp to normalise for gene length) for genes in the *sigB* operon that positively
 362 affect σ^B activity (*rsbV*, *rsbT* and *rsbU*) was considerably higher than for genes that act
 363 negatively (*rsbW* and *rsbX*). Indeed of all the genes we included in the analysis, *rsbU*
 364 was found to have the highest occurrence of PMSC (Fig. 8 A & B). Unexpectedly,
 365 *mazF* showed a high PMSC rate similar to *rsbV*, *rsbT* and *rsbU*. The gene *mazF*
 366 encodes for an endoribonuclease, a component of a toxin/anti-toxin system along with
 367 *mazE*, which is speculated to be an additional regulator for σ^B in *Staphylococcus aureus*

(45, 46) and have a positive effect in σ^B -dependent genes in *L. monocytogenes* in the presence of norfloxacin (47). The high PMSC rate in *mazF* may be associated with its putative positive regulation on σ^B thus it may also be subjected to the same selection pressure as σ^B positive regulators. Interestingly *rsbW*, which encodes the anti-sigma factor that negatively regulates σ^B activity, had no occurrence of PMSCs. As expected, essential genes such as *sigA*, which encodes the principal housekeeping sigma factor in *L. monocytogenes*, have a very low rate of PMSC occurrence, suggesting that this measure reflects the biological significance rather than just sequencing errors in the database. Interestingly, we found that the gene *inlA*, encoding for the internalin A was found to possess a very high PMSC rate per 100 bp (0.86% from a total of 4576 PMSCs found; data not shown). A previous study found that many of *L. monocytogenes* strains in lineage II possess PMSCs in *inlA* (48), for this reason we excluded this gene from Fig. 8. Interestingly, *inlB* which shares the same operon as *inlA*, also possess a high PMSC rate, although not as high as *inlA* (Fig. 8). Taken together these data indicate that within the published genome sequence data for *L. monocytogenes* there is a high occurrence of mutations that are predicted to reduce σ^B activity and low occurrence of mutations that would act to increase it.

385

386

387 Discussion

388 In this study we investigated the emergence and selection of spontaneous mutations
389 inactivating σ^B within populations of *L. monocytogenes*. We first identified these
390 mutations in a collection of *L. monocytogenes* “ringless” transposon mutant strains
391 whose response to visible light was altered, a phenotype that requires both the blue
392 light sensor RsbL and the stress-inducible sigma factor σ^B (32). One interpretation of
393 the mutants’ behaviour was that the transposon insertions somehow influenced the
394 signal transduction pathway leading to σ^B activation in response to light. Unexpectedly
395 we found that, in addition to the transposon insertions, all of the “ringless” mutant strains
396 we sequenced carried mutations in the *sigB* operon (*rsbS*, *rsbU* or *rsbV*), which were
397 predicted to produce premature stop codons in the corresponding coding sequences. In
398 addition to the “ringless” phenotype, the transposon mutant strains also exhibit reduced

399 acid tolerance and a marked decrease in σ^B activation when compared to the WT strain.
400 We conclude that the “ringless” and acid sensitive phenotypes of these mutant strains
401 are due to the presence of the *sigB* operon mutations rather than the transposon
402 insertions (32). These mutations most likely interfere with signal transduction through
403 the σ^B regulatory pathway since they are predicted to affect stressosome function
404 (*rsbS*), dephosphorylation of the anti-anti sigma factor RsbV (*rsbU*, which encodes a
405 phosphatase) or partner switching with the anti-sigma factor RsbW (*rsbV*). Indeed these
406 data provide additional genetic support for the existing model for σ^B activation in *L.*
407 *monocytogenes*, reviewed in (49, 50).

408
409
410 In previous studies, knockout deletions of the *rsbS*, *rsbV* or *rsbU* genes in both *L.*
411 *monocytogenes* and *B. subtilis* resulted in the impairment of the signal transduction and
412 reduced resistance against stress (14, 27-29, 31, 36, 40, 41). The premature stop
413 codons identified in this study do not result in the full loss of σ^B activity, since the σ^B -
414 dependent *P_{Imo2230}::egfp* reporter is still expressed in these transposon mutant strains
415 (Fig. 3) and this correlates with an intermediate acid tolerance phenotype, between that
416 of WT and the Δ *sigB* mutant strain (Fig. 1). It is noteworthy that no mutations were
417 detected in *sigB* itself, which could suggest that partial loss of function might be more
418 advantageous than complete loss of σ^B activity. The extent of the σ^B activity detected
419 appears to depend on which *sigB* operon frameshift allele is present. There is
420 significantly more σ^B activity present in strains carrying the frameshift allele encoding
421 RsbS-H23R than there is in the strains carrying either of the two *rsbV* frameshift alleles
422 (Fig. 3). This result suggests that loss of a functional RsbV has a greater impact on σ^B
423 activity than loss of RsbS. RsbV serves as an anti-anti sigma factor, whose role is to
424 sequester the anti-sigma factor RsbW during stress conditions, thereby releasing σ^B for
425 participation in transcription, while RsbS is an integral component of the stressosome
426 stress-sensing apparatus (16, 51). It is possible that some stress signals can still be
427 transduced through the pathway in the absence of RsbS but that this is less likely in the
428 absence of RsbV. In *B. subtilis* there is additional input into the pathway, which allows
429 energy stress to be sensed via the RsbP and RsbQ proteins, independently of the

430 stressosome (52). This pathway is not present in *L. monocytogenes* (29) but this does
431 not preclude some other stressosome-independent means of transducing stress signals
432 in this pathogen. Indeed there is evidence that even in the absence of RsbV some σ^B
433 activation can occur in some growth conditions (40). In *B. subtilis* RsbV-independent
434 activation of σ^B occurs at elevated temperatures (53) and in *L. monocytogenes* similar
435 observations have been made during growth at low temperatures (40, 54). The
436 possibility that RsbW could be regulated post-translationally, for example by proteolysis,
437 allowing an additional layer of control over σ^B is certainly worthy of further investigation.

438

439

440 **Emergence of mutated alleles within the *sigB* operon.**

441 The data presented here suggest an explanation for the common detection of mutations
442 in the *sigB* operon of *L. monocytogenes* (28, 33-36, 55), including an earlier study in our
443 own laboratory where an *rsbV* missense mutation arose during routine subculture (31).
444 Although the occurrence of *sigB* operon mutations has been reported by others, the
445 mechanism(s) that drives the selection of these mutations has remained elusive. Here
446 we show that loss of σ^B function confers a competitive advantage in conditions where
447 sub-lethal stress (in this case heat stress) prevails. The advantage is manifested both
448 as increased growth rate (Fig. 5) and increased competitiveness in mixed cultures (Fig.
449 6). Furthermore, the absence of *rsbX* which is predicted to increase σ^B activity confers a
450 competitive disadvantage under the same conditions (Fig. 7). Since a variety of the
451 protocols for genetically modifying *L. monocytogenes* include a step with prolonged
452 incubation at elevated temperature (typically 40-44°C) to prevent replication of plasmids
453 possessing a heat-sensitive origin of replication, used in order to encourage allele
454 integration into the chromosome (42, 56), it is possible that this provides the necessary
455 selective pressure to select mutant strains that negatively affect σ^B activity. Previous
456 studies have reported fast-growth phenotypes for *L. monocytogenes* mutant strains
457 lacking σ^B in stress conditions. In the presence of inhibitory doses of blue light *sigB*
458 mutant strains grow faster than the WT in liquid and solid media (31). In glucose-limited
459 conditions mutant strains lacking σ^B or the positively acting regulators RsbT or RsbV
460 were found to grow faster than the WT parent (29). A similar phenotype was observed

461 during growth at 3°C (30) and in conditions of osmotic stress (57). Indeed, there is
462 evidence in *B. subtilis* that mutant strains lacking σ^B can dominate the population in
463 nutrient-limited chemostats (58). Taken together with the findings presented in this
464 study, where a competitive advantage is demonstrated for mutant strains with reduced
465 σ^B activity in mixed populations, it seems likely that this phenotype is the reason for the
466 common emergence of mutations affecting σ^B activity during routine laboratory culture
467 of this pathogen.

468

469

470 An analysis of the over 22,000 *L. monocytogenes* publically available genome
471 assemblies revealed a high rate of premature stop codons within genes of the *sigB*
472 operon that positively regulate σ^B activity (Fig. 8), suggesting that there is some
473 selective pressure driving this process. It is not possible to determine precisely when
474 these PMSCs occurred and so it is unclear at present whether these mutations arose
475 during laboratory culture or whether they were already present in the wild isolates. It is
476 possible that conditions other than mild heat stress can confer a growth advantage on
477 mutant strains with reduced σ^B activity, as has been observed previously with light
478 stress and salt stress (57, 59). In *Escherichia coli* prolonged starvation during stationary
479 phase frequently results in mutant strains displaying a so-called GASP (Growth
480 Advantage in Stationary Phase) phenotype and these arise as a result of reduced
481 expression or activity of σ^S (RpoS), the sigma factor that controls the general stress
482 response in that organism (60, 61). Indeed mutations affecting *rpoS* frequently arise
483 during lab domestication of *E. coli* strains (62). A similar explanation has been
484 postulated to account for these observations in *E. coli*; namely the loss of σ^S function
485 arises when a fitness advantage accrues through the allocation of resources to growth
486 rather than to the costly general stress response (63, 64). Thus the phenomenon we
487 describe in this study is likely a reflection of a general biological principal where
488 competition within populations occasionally favours the emergence of variants that have
489 acquired a growth advantage at the expense of their ability to withstand potentially lethal
490 stress.

491

492

493 **σ^B deployment is a trade-off between growth and survival.**

494 Our study raises the important questions of how and why σ^B negatively affects growth
495 and competitiveness in mixed cultures. A number of possible, perhaps co-existing,
496 models could account for these phenomena. Firstly, it is possible that the expression of
497 the large σ^B regulon (approximately 300 genes), many components of which are actively
498 involved in homeostatic and repair functions, might represent a significant energy
499 burden on the cells. Freeing the cells from this energy burden could make more
500 resources available for biosynthesis and growth. Secondly it is possible that there is a
501 limited transcriptional capacity in the cell and the absence of σ^B allows the
502 housekeeping sigma factor (σ^A) to have greater access to the RNA polymerase core
503 enzyme, which leads to more efficient transcription of genes involved in growth-related
504 functions. This idea has been proposed previously to account for the emergence of
505 sigma S (*rpoS*) mutations in *E. coli* (65-67). Thirdly it is possible that σ^B actively restricts
506 growth, perhaps to ensure that protection and repair functions have sufficient time to
507 mitigate the damaging effects of stress. We recently provided evidence for this model as
508 we identified a sRNA under σ^B transcriptional control (Rli47) that acts to restrict the
509 biosynthesis of isoleucine, even when isoleucine is absent from the growth medium
510 (68). This somewhat surprising finding could provide evidence of deliberate σ^B -
511 controlled growth restriction. It is clear that further experiments will be needed to
512 specifically test these possibilities and establish the basis for the fast growth phenotype
513 associated with loss of σ^B activity.

514

515

516 Overall this study highlights the frequent occurrence of secondary mutations negatively
517 affecting σ^B activity in newly constructed strains of *L. monocytogenes*. It further
518 suggests that caution needs to be exercised by researchers to ensure that this issue
519 does not confound the interpretation of phenotypic data, especially where temperature
520 selection has been used during the strain construction. The availability and comparative
521 affordability of whole genome sequencing for bacteria makes it possible to routinely
522 sequence the genomes of newly constructed strains in order to avoid this issue and

indeed the availability of this data will make it easier to compare the behaviour of strains between groups. Finally, the study clearly illustrates the cost to the cell of deploying the σ^B -mediated general stress response; protection against stress is a resource-intensive process, but presumably the long-term survival benefits outweigh the short costs.

Materials and methods

Bacterial strains, plasmids and primers.

L. monocytogenes EGD-e and *E. coli* strains, primers and plasmids used for this study are listed on Table 1 and 3, respectively. Strains were grown in Brain Heart Infusion (BHI) broth or agar (LabM) at 37°C unless otherwise specified, at 150 rpm of constant shaking. Cells were grown for 16 h until stationary phase was reached. The following antibiotic concentrations were added to the media when required: chloramphenicol (Chl) 10 $\mu\text{g.mL}^{-1}$, erythromycin (Ery) 5 $\mu\text{g.mL}^{-1}$, tetracycline (Tet) 2.5 $\mu\text{g.mL}^{-1}$ for *L. monocytogenes* mutant strains; ampicillin (Amp) 100 $\mu\text{g.mL}^{-1}$ for *E. coli*.

Construction of genetically modified *L. monocytogenes*.

L. monocytogenes transposon mutant strains library was previously constructed by Tiensuu *et al.* (32). Electrocompetent cells were created as previously described (69). *L. monocytogenes* EGD-e ΔsigB mutant strain was constructed using a previously built shuttle vector pMAD:: ΔsigB (68). The shuttle vector pMAD:: ΔrsbX was generated by amplifying through PCR the *rsbX* flanking regions using primers *rsbX*-A and -B and *rsbX*-C and -D in separate reactions. Both flanks were joined together through splice overlap extension (SOE) PCR (69) using primers *rsbX*-A and -D. The resulting amplicon was digested with Sall and BglII and cloned into pMAD vector creating pMAD:: ΔrsbX . Confirmation of the construct was carried out by PCR using primers pMAD-U and pMAD-L. pMAD:: $\Delta\text{Imo0596}$ was constructed by digesting the artificially synthesized vector pEX-K168:: $\Delta\text{Imo0596}$ (Eurofins Genomics) with BamHI and Sall. The digestion product, containing 300 bp both upstream and downstream of *Imo0596* open reading frame, was ligated into pMAD vector creating pMAD:: $\Delta\text{Imo0596}$. Its construction was

554 verified by PCR with primers *Imo0596-A* and *Imo0596-B*. The mutagenic vectors,
 555 pMAD:: Δ *sigB*, pMAD:: Δ *rsbX* and pMAD:: Δ *Imo0596* were separately transformed into
 556 electrocompetent *L. monocytogenes* EGD-e. Transformants were selected from BHI
 557 agar supplemented with Ery growth at 30°C. Chromosomal integration of the vector was
 558 achieved by growing transformants at 39°C overnight in BHI supplemented with Ery.
 559 Cultures were plated in BHI agar containing the same antibiotic and X-gal (50 μ g.mL⁻¹)
 560 and colonies were allowed to growth at 41°C overnight. Blue colonies were growth at
 561 30°C overnight and 39°C for 3 hours. Serial dilutions were plated on BHI X-gal (50
 562 μ g.mL⁻¹) plates and grown at 30°C for two days. White colonies (indicating excision and
 563 loss of plasmid) were screened for erythromycin sensitivity and deletion knockouts of
 564 *sigB*, *rsbX* and *Imo0596* were checked by colony PCR using primers sigB-flank_F and
 565 sigB-flank_R, Imo0596-flank_F and Imo0596-flank_R and rsbX-flank_F and rsbX-
 566 flank_R, respectively. The σ^B reporter vector pKSV7-P_{*Imo2230*}::*egfp* (24) was
 567 transformed into electrocompetent *L. monocytogenes* transposon mutant strains.
 568 Electro-transformed colonies, were selected from BHI agar plates containing Chl and
 569 incubated at 30°C. The plasmid integration in the chromosome was achieved as
 570 previously described (24) by incubating fluorescent cells at 42°C. Plasmid's
 571 chromosomal integration occurred upstream of the original *Imo2230* promoter region of
 572 by homologues recombination. Integration was verified by PCR (using primers *egfp*-
 573 *Imo2230-F* integration and *egfp-Imo2230-F* integration).

576 **Acid tolerance (pH 2.5).**

577 Stationary phase cultures were pelleted down by centrifugation and resuspended in
 578 BHI, previously acidified with HCl 5 M until pH 2.5. Resuspensions were incubated in a
 579 water-bath at 37°C for 120 min. Samples were taken at 0, 30, 60 and 120 min, serial
 580 diluted from 10⁻⁷ to 10⁻² in PBS and plated in BHI agar plates. Plates were then
 581 incubated at 37°C for 24 hours and colonies were counted. A minimum of three
 582 biological replicates were made.

585 **Whole genome sequencing (WGS).**

586 Transposon mutant strains genomic DNA was extracted using DNeasy[®] Blood & Tissue
587 Kit (Qiagen) following the manufacturer recommendations. Purified genomic DNA was
588 sent to MicrobesNG for WGS. The obtained trimmed reads were used for SNP
589 identification analysis performed in Breseq (70). The transposon sequence was located
590 in each transposon mutant strain by using the contig reads on Mauve - Multiple
591 Genome Alignment (71). *L. monocytogenes* EGD-e (NCBI Reference Sequence:
592 NC_003210.1; (https://www.ncbi.nlm.nih.gov/nuccore/NC_003210.1) genomic
593 sequence was used as reference genome in both analysis.

594
595
596 **Microscopic quantification of eGFP fluorescence.**

597 Cells containing the eGFP σ^B -reporter (pKSV7-*P_{Imo2230}::egfp*) integrated in *L.*
598 *monocytogenes* chromosome were grown for 16 h to stationary phase. Cultures were
599 mixed in 1:1 volume of ice cold methanol/ethanol 1:1 (v/v) mixture and placed at -20°C
600 for 10 min. The mixtures were centrifuged afterwards at 10,000 x *g* for 10 min at 4°C.
601 The supernatant was removed and the pellet was resuspended in ice cold PBS and
602 cells were further adjusted to OD₆₀₀ of 1. Fluorescence microscopy was performed in a
603 Nikon Eclipse E600 microscope by using a B-2A filter covering the eGFP excitation and
604 emission wavelengths. A total of 5 images per biological replicate were taken across
605 different fields of the slide. Images were digitally captured through a CCD camera
606 attached to the microscope. Relative fluorescence intensities were reported after
607 automated image processing of multiple fields with ImageJ 1.44 software (72) with
608 appropriate manipulations as described by others (73, 74).

609
610
611 **SDS-PAGE and Western-Blot.**

612 The total protein fraction were extracted from stationary phase cultures grown at 37°C.
613 Tet was added to the cultures and centrifuged at 9,000 x *g* for 15 min at 4°C. Cells were
614 resuspended in Sonication buffer containing 13 mM Tris-HCl, 0.123 mM EDTA and
615 10.67 mM MgCl₂ adjusted to pH 8.0. Cell suspensions were digested with 1 mg.mL⁻¹

616 lysozyme (Sigma-Aldrich) for 30 min and centrifuged again. Pellets were resuspended
 617 in sonication buffer containing 1% (v/v) protease inhibitor cocktail (P2714, Sigma-
 618 Aldrich). Resuspensions were then transferred into cryotubes containing zirconia/silica
 619 beads (Thistle Scientific) and beadbeated in FastPrep[®]-24 at a speed of 6 m.s⁻¹ for 40 s
 620 twice. Lysates were centrifuged for 13000 x *g* for 30 min at 4°C and the supernatant
 621 recovered. Total protein quantification was performed through DC Protein Assay (Bio-
 622 Rad) using the manufacturer recommendations. Protein extracts were normalized to 0.8
 623 mg.mL⁻¹ of total protein concentration and 12 µL of each sample was separated by
 624 SDS-PAGE (15% acrylamide/bis-acrylamide) along with the PageRuler[™] Plus
 625 Prestained (Thermo Scientific). Separated protein was transferred into a Polyvinylidene
 626 difluoride (PVDF) membrane and blocked with TBS supplemented with 3% (w/v) skim
 627 milk power (Sigma). SDS-PAGE gels were further stained with GelCode[®] Blue Staining
 628 Reagent (Thermo Scientific) and destained with destaining solution (20% acetic acid
 629 and 10% methanol) (Fig. S3). For immunoblots, rabbit polyclonal IgG anti-GFP (FL)
 630 (Santa Cruz[®] Biotechnology) and rabbit polyclonal IgG anti-σ^B (40), were diluted 1:500
 631 and 1:1500, respectively, in TBS. The rabbit polyclonal IgG anti-RsbT were diluted
 632 1:5000 in SignalBoost[™] Immunoreaction Enhancer Kit (Merck). Secondary antibodies
 633 mouse anti-rabbit IgG-HRP (Santa Cruz[®] Biotechnology) were diluted 1:6500 in TBS or
 634 SignalBoost[™] Immunoreaction Enhancer Kit (Merck) when required. Blots were
 635 visualized on Odyssey[®]Fc Imaging System (LI-COR Biosciences).

636

637

638 **Growth kinetics.**

639 Stationary phase cells grown in BHI at 37°C of *L. monocytogenes* WT, Δ*sigB*, B14:A6
 640 and 2RsbU (E103K) were adjusted to an OD₆₀₀ of 0.05 and grown in BHI at 30°C, 37°C,
 641 40°C and 42°C. OD₆₀₀ of each culture was measured every hour for 12 hours. Growth
 642 rates were calculated by determining the slope during the transition into the stationary
 643 phase, between 4 and 5 hours at 37°C, 40°C and 42°C and between 6 and 7 at 30°C. A
 644 minimum of 3 biological replicates were made.

645

646

647 **Competition experiments.**

648 *L. monocytogenes* WT, the “ringless” 2RsbU (E103K) and ring-forming control B14:A6
649 were grown in BHI at 37°C for 16 hours until stationary phase was reached. Cultures
650 were adjusted to an initial OD₆₀₀ of 0.05 in fresh BHI in final ratios of 1:1000, 1:1 and
651 1000:1 of mixtures of WT with 2RsbU (E103K) and WT with B14:A6, at the indicated
652 temperatures. Passages were made every 24 hours by diluting 1:100 into fresh BHI.
653 Samples were taken and diluted to 10⁻⁷ in PBS in every passage and plated in both BHI
654 and BHI supplemented with erythromycin to distinguish non-erythromycin resistant WT
655 from the resistant transposon mutant strain colonies and incubated at 37°C. Colonies
656 were counted after 24 hours of incubation. Ratios were calculated by subtracting the
657 number of erythromycin resistant colonies to the total number of colonies. Competitions
658 cultures of WT vs. $\Delta sigB$ and WT vs. $\Delta rsbX$ were performed as described above with
659 the following modifications. Cultures were incubated in BHI agar plates for 24 hours at
660 37°C. Differences in colony morphology were used to distinguish WT from both $\Delta rsbX$
661 and $\Delta sigB$ strains. The colony size of $\Delta rsbX$ colonies was significantly smaller than the
662 WT strain. For WT vs. $\Delta sigB$ competitions, BHI plates were further incubated at 30°C for
663 7 days and strains were distinguished by differences in colony coloration. We observed
664 that the WT colonies showed whiter coloration in comparison with the $\Delta sigB$.
665 Confirmation of WT and $\Delta sigB$ mutant strain colonies were carried out through colony
666 PCR, by amplifying the flanking regions of *sigB* (using primers *sigB*-flank_F and *sigB*-
667 flank_R). A total of 60 colonies, 30 of each coloration were tested using MyTaq™ DNA
668 Polymerase Kit (Bioline). WT and $\Delta rsbX$ mutant strain were also confirmed via the same
669 method by amplifying the flanking regions of *rsbX* (using primers *rsbX*-flank_F and
670 *rsbX*-flank_R) of a total of 24 colonies, 12 WT and 12 $\Delta rsbX$. This method enables the
671 WT to be distinguished from the $\Delta sigB$ with a precision of 98.3% and the WT from the
672 $\Delta rsbX$ with 100%.

673

674

675 ***In silico* analysis of premature stop codon (PMSC) occurrence rates.**

676 A DNA BLAST database was constructed for 22,340 *L. monocytogenes* genome
677 assemblies available from NCBI database (182 complete genomes, 45 chromosomal

678 genomes and 22,113 assembly scaffold or contigs, accessed in July 5th 2019). DNA
679 coding sequences of 41 genes of interest, including all 10 genes from the *sigB* operon,
680 2 genes immediately downstream from the *sigB* operon, 7 housekeeping genes used in
681 Multilocus Sequencing Typing (MLST) (75), 4 genes encoding for *rsbR* paralogues, 3
682 sigma factor genes, 5 virulence factors and 10 genes intervening in several different
683 metabolic pathways were extracted from *L. monocytogenes* EGD-e strain and used as
684 query sequences. BLASTn was performed with each query sequence against all 22,340
685 DNA databases and then the DNA sequences were extracted for the closest match.
686 Genes were considered absent or incomplete in a given genome assembly when either
687 (i) the: BLASTn top hit is empty; (ii) the start or end of subject sequence is less than 20
688 bp from end or start of contig in which subject sequence was found; or (iii) the subject
689 sequence is shorter than query sequence by ≥ 25 bp. Otherwise the gene was
690 considered present and complete in genome assembly and then translated with
691 Biopython (76) according to bacterial translate table to determine the position of stop
692 codons and identify PMSCs (defined as codons that truncate the gene length to less
693 than 90% the length of the gene in the reference strain EGD-e). For each gene
694 analysed, the occurrence rate of PMSCs was calculated as a rate normalised to 100 bp
695 to account for the different gene lengths in the analysis.

696

697

698 **Ring formation phenotype.**

699 Overnight cultures grown at 30°C and 2 μ L were spotted onto BHI soft agar plates
700 (0.3% w/v agar No. 2) previously dried in a laminar flow hood for 10 min. Plates were
701 incubated at 30°C for 4 days either in constant dark or exposed to cycles of 12 h of light
702 and dark in a blue-light array apparatus with an average intensity of 0.2 mW.cm⁻².
703 Photographs of the grown plates were acquired using the Syngene GBox – Chemi 16
704 Bio Imaging System.

705

706

707 **RNA extraction and RT-qPCR.**

708 Overnight cultures of *L. monocytogenes* WT, $\Delta sigB$ and $\Delta Imo0596$ mutant strains were
 709 grown in BHI were adjusted to an initial OD₆₀₀ of 0.05 in fresh BHI and allowed to grow
 710 until mid-log phase was reached (OD₆₀₀ = 0.8) or allowed to grow overnight until
 711 stationary phase. Transcription was stopped by diluting the cultures in RNA^{later}[®]
 712 (Sigma) in 1:5 ratio. Total RNA was extracted using RNeasy Mini Kit (Qiagen) by
 713 following the manufacturer recommendations. Cell disruption was achieved by bead-
 714 beating in FastPrep with the same parameters as mention before. Total DNA was
 715 digested with TURBO DNA-free™ (Invitrogen) digestion by following the manufacturer
 716 recommendations. RNA integrity was verified through 0.7% agarose gel
 717 electrophoresis. cDNA was synthesised with SuperScript™ IV First-Strand Synthesis
 718 System (Invitrogen) following the manufacturer recommendations and further quantified
 719 in Qubit™ (Invitrogen). RT-qPCR was performed using QuantiTect™ SYBR Green PCR
 720 Kit (Qiagen) and primer for the target genes (Table 3). Primers efficiency for the target
 721 genes 16s, *Imo2230*, *sreB* and *Imo0596* were determinate using purified *L.*
 722 *monocytogenes* genomic DNA. Samples were analysed on LightCycler® 480 System
 723 (Roche) with the following parameters, 95°C for 15 min, 45 cycles of 15 s at 95°C, 15 s
 724 at 53°C and 30 s at 72°C, a melting curve was drawn for 5 s at 95°C, 1 min at 55°C
 725 followed by increases of 0.11°C.s⁻¹ until 95°C, and a cooling for 30 s at 40°C. Cycle
 726 quantification values were calculated by the software LightCycler® 480 Software
 727 version 1.5.1 (Roche) and the Pfaffl relative expression formula (77, 78). The
 728 expression of the 16s rDNA was used as reference gene. Three biological replicates,
 729 each in technical duplicates were performed. Results are expressed in Log₂ relative
 730 expression ratio normalized against the WT strain.

731

732

733 **Statistical analysis.**

734 Student's *t*-test analysis was performed on GraphPad Prism 8.

735

736

737 **Acknowledgements**

738 This project has received funding from the European Union's Horizon 2020 research
 739 and innovation programme under the Marie Skłodowska-Curie grant agreement No.
 740 721456. Jialun Wu was funded by the Department of Agriculture, Food and the Marine
 741 (17/F/244).
 742 The authors wish to acknowledge Nicholas Waters for the help in scripting.

743

744

745 References

- 746 1. Mylonakis E, Paliou M, Hohmann EL, Calderwood SB, Wing EJ. 2002. Listeriosis
 747 during pregnancy: a case series and review of 222 cases. *Medicine* 81:260-269.
- 748 2. Farber J, Peterkin P. 1991. *Listeria monocytogenes*, a food-borne pathogen.
 749 *Microbiology and Molecular Biology Reviews* 55:476-511.
- 750 3. Barbuddhe SB, Chakraborty T. 2009. *Listeria* as an enteroinvasive
 751 gastrointestinal pathogen, p 173-195, *Molecular mechanisms of bacterial*
 752 *infection via the gut*. Springer.
- 753 4. Gandhi M, Chikindas ML. 2007. *Listeria*: a foodborne pathogen that knows how
 754 to survive. *International journal of food microbiology* 113:1-15.
- 755 5. Jensen VB, Harty JT, Jones BD. 1998. Interactions of the Invasive
 756 Pathogens *Salmonella typhimurium*, *Listeria monocytogenes*, and *Shigella*
 757 *flexneri* with M Cells and Murine Peyer's Patches. *Infection and immunity*
 758 66:3758-3766.
- 759 6. Liu Y, Orsi RH, Boor KJ, Wiedmann M, Guariglia-Oropeza V. 2017. Home alone:
 760 elimination of all but one alternative sigma factor in *Listeria monocytogenes*
 761 allows prediction of new roles for σ B. *Frontiers in microbiology* 8:1910.
- 762 7. Chaturongakul S, Raengpradub S, Palmer ME, Bergholz TM, Orsi RH, Hu Y,
 763 Ollinger J, Wiedmann M, Boor KJ. 2011. Transcriptomic and phenotypic analyses
 764 identify coregulated, overlapping regulons among PrfA, CtsR, HrcA, and the
 765 alternative sigma factors σ B, σ C, σ H, and σ L in *Listeria monocytogenes*. *Applied*
 766 *and environmental microbiology* 77:187-200.
- 767 8. Sleator RD, Watson D, Hill C, Gahan CG. 2009. The interaction between *Listeria*
 768 *monocytogenes* and the host gastrointestinal tract. *Microbiology* 155:2463-2475.
- 769 9. Kim H, Marquis H, Boor KJ. 2005. σ B contributes to *Listeria monocytogenes*
 770 invasion by controlling expression of *inlA* and *inlB*. *Microbiology (Reading,*
 771 *England)* 151:3215.
- 772 10. Wise AA, Price CW. 1995. Four additional genes in the *sigB* operon of *Bacillus*
 773 *subtilis* that control activity of the general stress factor sigma B in response to
 774 environmental signals. *Journal of bacteriology* 177:123-133.
- 775 11. Toledo-Arana A, Dussurget O, Nikitas G, Sesto N, Guet-Revillet H, Balestrino D,
 776 Loh E, Gripenland J, Tiensuu T, Vaitkevicius K. 2009. The *Listeria* transcriptional
 777 landscape from saprophytism to virulence. *Nature* 459:950.

- 778 12. Ferreira A, Gray M, Wiedmann M, Boor KJ. 2004. Comparative genomic analysis
779 of the sigB operon in *Listeria monocytogenes* and in other Gram-positive
780 bacteria. *Current microbiology* 48:39-46.
- 781 13. Boylan SA, Rutherford A, Thomas SM, Price CW. 1992. Activation of *Bacillus*
782 *subtilis* transcription factor sigma B by a regulatory pathway responsive to
783 stationary-phase signals. *Journal of Bacteriology* 174:3695-3706.
- 784 14. Benson AK, Haldenwang WG. 1992. Characterization of a regulatory network
785 that controls sigma B expression in *Bacillus subtilis*. *Journal of Bacteriology*
786 174:749-757.
- 787 15. Marles-Wright J, Lewis RJ. 2010. The stressosome: molecular architecture of a
788 signalling hub. Portland Press Limited.
- 789 16. Pané-Farré J, Quin MB, Lewis RJ, Marles-Wright J. 2017. Structure and function
790 of the stressosome signalling hub, p 1-41, *Macromolecular Protein Complexes*.
791 Springer.
- 792 17. Impens F, Rolhion N, Radoshevich L, Bécavin C, Duval M, Mellin J, del Portillo
793 FG, Pucciarelli MG, Williams AH, Cossart P. 2017. N-terminomics identifies
794 Prli42 as a membrane miniprotein conserved in Firmicutes and critical for
795 stressosome activation in *Listeria monocytogenes*. *Nature microbiology* 2:17005.
- 796 18. Martinez L, Reeves A, Haldenwang W. 2010. Stressosomes formed in *Bacillus*
797 *subtilis* from the RsbR protein of *Listeria monocytogenes* allow σ B activation
798 following exposure to either physical or nutritional stress. *Journal of bacteriology*
799 192:6279-6286.
- 800 19. Ondrusch N, Kreft J. 2011. Blue and red light modulates SigB-dependent gene
801 transcription, swimming motility and invasiveness in *Listeria monocytogenes*.
802 *PloS one* 6:e16151.
- 803 20. Delumeau O, Chen C-C, Murray JW, Yudkin MD, Lewis RJ. 2006. High-
804 molecular-weight complexes of RsbR and paralogues in the environmental
805 signaling pathway of *Bacillus subtilis*. *Journal of bacteriology* 188:7885-7892.
- 806 21. Gaidenko TA, Yang X, Lee YM, Price CW. 1999. Threonine phosphorylation of
807 modulator protein RsbR governs its ability to regulate a serine kinase in the
808 environmental stress signaling pathway of *Bacillus subtilis* 1. *Journal of*
809 *molecular biology* 288:29-39.
- 810 22. Kim T-J, Gaidenko TA, Price CW. 2004. A multicomponent protein complex
811 mediates environmental stress signaling in *Bacillus subtilis*. *Journal of molecular*
812 *biology* 341:135-150.
- 813 23. Yang X, Kang CM, Brody MS, Price CW. 1996. Opposing pairs of serine protein
814 kinases and phosphatases transmit signals of environmental stress to activate a
815 bacterial transcription factor. *Genes & development* 10:2265-2275.
- 816 24. Utratna M, Cosgrave E, Baustian C, Ceredig R, O'Byrne C. 2012. Development
817 and optimization of an EGFP-based reporter for measuring the general stress
818 response in *Listeria monocytogenes*. *Bioengineered* 3:93-103.
- 819 25. Kang CM, Vijay K, Price CW. 1998. Serine kinase activity of a *Bacillus subtilis*
820 switch protein is required to transduce environmental stress signals but not to
821 activate its target PP2C phosphatase. *Molecular microbiology* 30:189-196.

- 822 26. Kim T-J, Gaidenko TA, Price CW. 2004. In vivo phosphorylation of partner
823 switching regulators correlates with stress transmission in the environmental
824 signaling pathway of *Bacillus subtilis*. *Journal of bacteriology* 186:6124-6132.
- 825 27. Shin J-H, Brody MS, Price CW. 2010. Physical and antibiotic stresses require
826 activation of the RsbU phosphatase to induce the general stress response in
827 *Listeria monocytogenes*. *Microbiology* 156:2660.
- 828 28. Tran V, Geraci K, Midili G, Satterwhite W, Wright R, Bonilla CY. 2018. Resilience
829 to oxidative and nitrosative stress is mediated by the stressosome, RsbP and
830 SigB in *Bacillus subtilis*. *bioRxiv*:460303.
- 831 29. Chaturongakul S, Boor KJ. 2004. RsbT and RsbV contribute to σ B-dependent
832 survival under environmental, energy, and intracellular stress conditions in
833 *Listeria monocytogenes*. *Applied and environmental microbiology* 70:5349-5356.
- 834 30. Brøndsted L, Kallipolitis BH, Ingmer H, Knöchel S. 2003. kdpE and a putative
835 RsbQ homologue contribute to growth of *Listeria monocytogenes* at high
836 osmolarity and low temperature. *FEMS microbiology letters* 219:233-239.
- 837 31. O'Donoghue B. 2016. A molecular genetic investigation into stress sensing in the
838 food-borne pathogen *Listeria Monocytogenes*: roles for RsbR and its paralogues,
839 Doctoral Thesis. National University of Ireland, Galway, Ireland. URL:
840 <http://hdl.handle.net/10379/6310>.
- 841 32. Tiensuu T, Andersson C, Rydén P, Johansson J. 2013. Cycles of light and dark
842 co-ordinate reversible colony differentiation in *Listeria monocytogenes*. *Molecular*
843 *microbiology* 87:909-924.
- 844 33. Hauf S, Herrmann J, Miethke M, Gibhardt J, Commichau FM, Müller R, Fuchs S,
845 Halbedel S. 2019. Aurantimycin resistance genes contribute to survival of *Listeria*
846 *monocytogenes* during life in the environment. *Molecular microbiology*.
- 847 34. Hingston P, Chen J, Dhillon BK, Laing C, Bertelli C, Gannon V, Tasara T, Allen
848 K, Brinkman FS, Truelstrup Hansen L. 2017. Genotypes associated with *Listeria*
849 *monocytogenes* isolates displaying impaired or enhanced tolerances to cold, salt,
850 acid, or desiccation stress. *Frontiers in microbiology* 8:369.
- 851 35. Asakura H, Kawamoto K, Okada Y, Kasuga F, Makino S-i, Yamamoto S, Igimi S.
852 2012. Intrahost passage alters SigB-dependent acid resistance and host cell-
853 associated kinetics of *Listeria monocytogenes*. *Infection, Genetics and Evolution*
854 12:94-101.
- 855 36. Quereda JJ, Pucciarelli MG, Botello-Morte L, Calvo E, Carvalho F, Bouchier C,
856 Vieira A, Mariscotti JF, Chakraborty T, Cossart P. 2013. Occurrence of mutations
857 impairing sigma factor B (SigB) function upon inactivation of *Listeria*
858 *monocytogenes* genes encoding surface proteins. *Microbiology* 159:1328-1339.
- 859 37. Loh E, Dussurget O, Gripenland J, Vaitkevicius K, Tiensuu T, Mandin P, Repoila
860 F, Buchrieser C, Cossart P, Johansson J. 2009. A trans-acting riboswitch
861 controls expression of the virulence regulator PrfA in *Listeria monocytogenes*.
862 *Cell* 139:770-779.
- 863 38. Rauch M, Luo Q, Müller-Altroch S, Goebel W. 2005. SigB-dependent in vitro
864 transcription of prfA and some newly identified genes of *Listeria monocytogenes*
865 whose expression is affected by PrfA in vivo. *Journal of bacteriology* 187:800-
866 804.

- 867 39. Utratna M, Shaw I, Starr E, O'Byrne CP. 2011. Rapid, transient, and proportional
868 activation of σ^B in response to osmotic stress in *Listeria monocytogenes*. *Appl*
869 *Environ Microbiol* 77:7841-7845.
- 870 40. Utratna M, Cosgrave E, Baustian C, Ceredig RH, O'Byrne CP. 2014. Effects of
871 growth phase and temperature on activity within a *Listeria monocytogenes*
872 population: evidence for RsbV-independent activation of σ^B at refrigeration
873 temperatures. *BioMed research international* 2014.
- 874 41. Zhang Z, Meng Q, Qiao J, Yang L, Cai X, Wang G, Chen C, Zhang L. 2013.
875 RsbV of *Listeria monocytogenes* contributes to regulation of environmental stress
876 and virulence. *Archives of microbiology* 195:113-120.
- 877 42. Cao M, Bitar AP, Marquis H. 2007. A mariner-based transposition system for
878 *Listeria monocytogenes*. *Appl Environ Microbiol* 73:2758-2761.
- 879 43. Chen CC, Lewis RJ, Harris R, Yudkin MD, Delumeau O. 2003. A supramolecular
880 complex in the environmental stress signalling pathway of *Bacillus subtilis*.
881 *Molecular microbiology* 49:1657-1669.
- 882 44. Eymann C, Schulz S, Gronau K, Becher D, Hecker M, Price CW. 2011. In vivo
883 phosphorylation patterns of key stressosome proteins define a second feedback
884 loop that limits activation of *Bacillus subtilis* σ^B . *Molecular microbiology* 80:798-
885 810.
- 886 45. Fu Z, Tamber S, Memmi G, Donegan NP, Cheung AL. 2009. Overexpression of
887 MazFsa in *Staphylococcus aureus* induces bacteriostasis by selectively targeting
888 mRNAs for cleavage. *Journal of bacteriology* 191:2051-2059.
- 889 46. Schuster CF, Mechler L, Nolle N, Krismer B, Zelder M-E, Götz F, Bertram R.
890 2015. The MazEF toxin-antitoxin system alters the β -lactam susceptibility of
891 *Staphylococcus aureus*. *PLoS One* 10:e0126118.
- 892 47. Curtis TD, Takeuchi I, Gram L, Knudsen GM. 2017. The Influence of the
893 Toxin/Antitoxin mazEF on Growth and Survival of *Listeria monocytogenes* under
894 Stress. *Toxins* 9:31.
- 895 48. Orsi R, Ripoll D, Yeung M, Nightingale K, Wiedmann M. 2007. Recombination
896 and positive selection contribute to evolution of *Listeria monocytogenes* *inA*.
897 *Microbiology* 153:2666-2678.
- 898 49. Dorey A, Marinho C, Piveteau P, O'Byrne C. 2019. Role and regulation of the
899 stress activated sigma factor sigma B (σ^B) in the saprophytic and host-
900 associated life stages of *Listeria monocytogenes*. *Advances in applied*
901 *microbiology* 106:1-48.
- 902 50. Tiensuu T, Guerreiro DN, Oliveira AH, O'Byrne C, Johansson J. 2019. Flick of a
903 switch: regulatory mechanisms allowing *Listeria monocytogenes* to transition
904 from a saprophyte to a killer. *Microbiology* 165:819-833.
- 905 51. Marles-Wright J, Lewis RJ. 2008. The *Bacillus subtilis* stressosome: A signal
906 integration and transduction hub. *Communicative & integrative biology* 1:182-
907 184.
- 908 52. Voelker U, Voelker A, Haldenwang WG. 1996. Reactivation of the *Bacillus*
909 *subtilis* anti-sigma B antagonist, RsbV, by stress- or starvation-induced
910 phosphatase activities. *Journal of bacteriology* 178:5456-5463.
- 911 53. Holtmann G, Brigulla M, Steil L, Schütz A, Barnekow K, Völker U, Bremer E.
912 2004. RsbV-independent induction of the SigB-dependent general stress regulon

- 913 of *Bacillus subtilis* during growth at high temperature. *Journal of bacteriology*
 914 186:6150-6158.
- 915 54. Brigulla M, Hoffmann T, Krisp A, Völker A, Bremer E, Völker U. 2003. Chill
 916 induction of the SigB-dependent general stress response in *Bacillus subtilis* and
 917 its contribution to low-temperature adaptation. *Journal of bacteriology* 185:4305-
 918 4314.
- 919 55. Hsu C-Y, Cairns L, Hobley L, Abbott J, O'Byrne C, Stanley-Wall NR. 2020.
 920 Genomic differences between *Listeria monocytogenes* EGDe isolates reveals
 921 crucial roles for SigB and wall rhamnosylation in biofilm formation. *Journal of*
 922 *Bacteriology*.
- 923 56. Arnaud M, Chastanet A, Débarbouillé M. 2004. New vector for efficient allelic
 924 replacement in naturally nontransformable, low-GC-content, gram-positive
 925 bacteria. *Appl Environ Microbiol* 70:6887-6891.
- 926 57. Abram F, Starr E, Karatzas K-AG, Matlawska-Wasowska K, Boyd A, Wiedmann
 927 M, Boor K, Connally D, O'Byrne C. 2008. Identification of components of the
 928 sigma B regulon in *Listeria monocytogenes* that contribute to acid and salt
 929 tolerance. *Applied and environmental microbiology* 74:6848-6858.
- 930 58. Schweder T, Kolyschcow A, Völker U, Hecker M. 1999. Analysis of the
 931 expression and function of the σ B-dependent general stress regulon of *Bacillus*
 932 *subtilis* during slow growth. *Archives of microbiology* 171:439-443.
- 933 59. O'Donoghue B, NicAogáin K, Bennett C, Conneely A, Tiensuu T, Johansson J,
 934 O'Byrne C. 2016. Blue-light inhibition of *Listeria monocytogenes* growth is
 935 mediated by reactive oxygen species and is influenced by σ B and the blue-light
 936 sensor Lmo0799. *Applied and environmental microbiology* 82:4017-4027.
- 937 60. Finkel SE. 2006. Long-term survival during stationary phase: evolution and the
 938 GASP phenotype. *Nature Reviews Microbiology* 4:113.
- 939 61. Zambrano MM, Kolter R. 1996. GASping for life in stationary phase. *Cell* 86:181-
 940 184.
- 941 62. Liu B, Eydallin G, Maharjan RP, Feng L, Wang L, Ferenci T. 2017. Natural
 942 *Escherichia coli* isolates rapidly acquire genetic changes upon laboratory
 943 domestication. *Microbiology* 163:22-30.
- 944 63. Maharjan R, Nilsson S, Sung J, Haynes K, Beardmore RE, Hurst LD, Ferenci T,
 945 Gudelj I. 2013. The form of a trade-off determines the response to competition.
 946 *Ecology letters* 16:1267-1276.
- 947 64. Gudelj I, Weitz JS, Ferenci T, Claire Horner-Devine M, Marx CJ, Meyer JR,
 948 Forde SE. 2010. An integrative approach to understanding microbial diversity:
 949 from intracellular mechanisms to community structure. *Ecology letters* 13:1073-
 950 1084.
- 951 65. Farewell A, Kvint K, Nyström T. 1998. Negative regulation by RpoS: a case of
 952 sigma factor competition. *Molecular microbiology* 29:1039-1051.
- 953 66. Notley-McRobb L, King T, Ferenci T. 2002. rpoS mutations and loss of general
 954 stress resistance in *Escherichia coli* populations as a consequence of conflict
 955 between competing stress responses. *Journal of bacteriology* 184:806-811.
- 956 67. Nyström T. 2004. MicroReview: Growth versus maintenance: a trade-off dictated
 957 by RNA polymerase availability and sigma factor competition? *Molecular*
 958 *microbiology* 54:855-862.

- 959 68. Marinho CM, Dos Santos PT, Kallipolitis BH, Johansson J, Ignatov D, Guerreiro
960 DN, Piveteau P, O'Byrne CP. 2019. The σ B-dependent regulatory sRNA Rli47
961 represses isoleucine biosynthesis in *Listeria monocytogenes* through a direct
962 interaction with the *ilvA* transcript. *RNA biology*:1-15.
- 963 69. Monk IR, Gahan CG, Hill C. 2008. Tools for functional postgenomic analysis of
964 *Listeria monocytogenes*. *Appl Environ Microbiol* 74:3921-34.
- 965 70. Deatherage DE, Barrick JE. 2014. Identification of mutations in laboratory-
966 evolved microbes from next-generation sequencing data using breseq, p 165-
967 188, *Engineering and analyzing multicellular systems*. Springer.
- 968 71. Darling AC, Mau B, Blattner FR, Perna NT. 2004. Mauve: multiple alignment of
969 conserved genomic sequence with rearrangements. *Genome research* 14:1394-
970 1403.
- 971 72. Collins TJ. 2007. ImageJ for microscopy. *BioTechniques* 43:S25-S30.
- 972 73. Hamilton N. 2009. Quantification and its applications in fluorescent microscopy
973 imaging. *Traffic* 10:951-961.
- 974 74. Selinummi J, Seppälä J, Yli-Harja O, Puhakka JA. 2005. Software for
975 quantification of labeled bacteria from digital microscope images by automated
976 image analysis. *Biotechniques* 39:859-863.
- 977 75. Salcedo C, Arreaza L, Alcalá B, De La Fuente L, Vazquez J. 2003. Development
978 of a multilocus sequence typing method for analysis of *Listeria monocytogenes*
979 clones. *Journal of clinical microbiology* 41:757-762.
- 980 76. Cock PJ, Antao T, Chang JT, Chapman BA, Cox CJ, Dalke A, Friedberg I,
981 Hamelryck T, Kauff F, Wilczynski B. 2009. Biopython: freely available Python
982 tools for computational molecular biology and bioinformatics. *Bioinformatics*
983 25:1422-1423.
- 984 77. Pfaffl MW. 2001. A new mathematical model for relative quantification in real-
985 time RT-PCR. *Nucleic acids research* 29:e45-e45.
- 986 78. Pfaffl M, Georgieva TM, Georgiev IP, Ontsouka E, Hageleit M, Blum J. 2002.
987 Real-time RT-PCR quantification of insulin-like growth factor (IGF)-1, IGF-1
988 receptor, IGF-2, IGF-2 receptor, insulin receptor, growth hormone receptor, IGF-
989 binding proteins 1, 2 and 3 in the bovine species. *Domestic animal endocrinology*
990 22:91-102.
- 991 79. den Dunnen JT, Dalgleish R, Maglott DR, Hart RK, Greenblatt MS, McGowan-
992 Jordan J, Roux AF, Smith T, Antonarakis SE, Taschner PE. 2016. HGVS
993 recommendations for the description of sequence variants: 2016 update. *Human*
994 *mutation* 37:564-569.

997 **Figures captions**
998

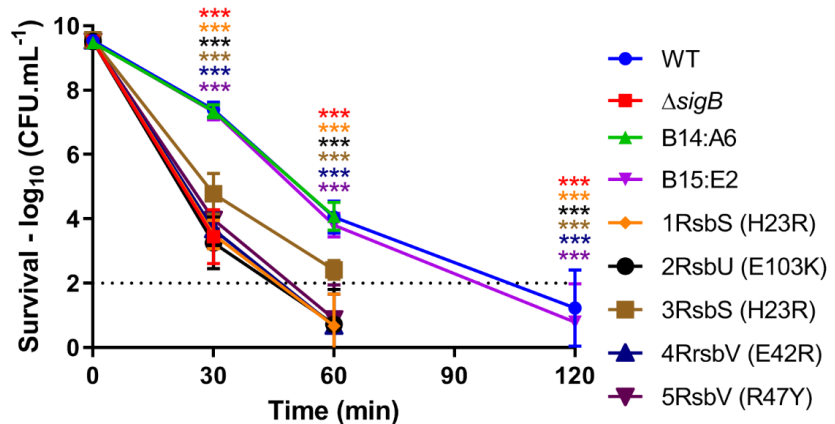


FIG 1 “Ringless” transposon mutant strains have acid sensitive phenotypes. Stationary phase cultures grown in BHI at 37°C before being challenged in acidified BHI (pH 2.5) at 37°C. At 0, 30, 50 and 120 min, samples were taken for viable counts measurement. Dotted line represents the detection threshold. Each marker represents the measurement average of three independent biological replicates performed, with the respective standard deviation. Statistical analysis was performed using a paired Student *t*-test (***) = *p*-value < 0.001).

999
1000

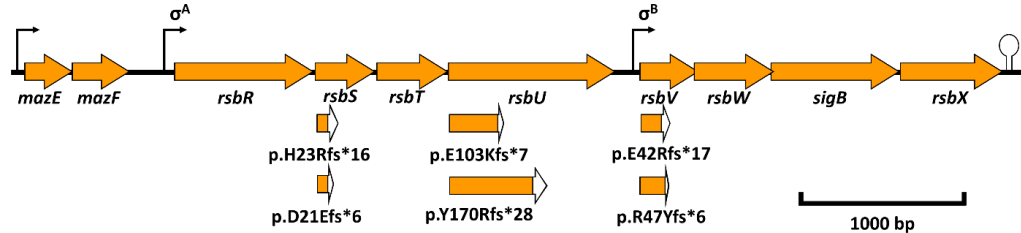


FIG 2 Locations of the frameshift mutations in the *sigB* operon. Layout of the *sigB* operon with the respective promoter regions and terminator. Each arrow representing the ORF of *mazE*, *mazF*, *rsbR*, *rsbS*, *rsbT*, *rsbU*, *rsbV*, *rsbW*, *sigB* and *rsbX* with the respective location of the identified mutations. White sections of the ORF represent the alternate reading frame produced by the frameshift mutations in *rsbS*, *rsbU* and *rsbV* until a PMSC is encoded.

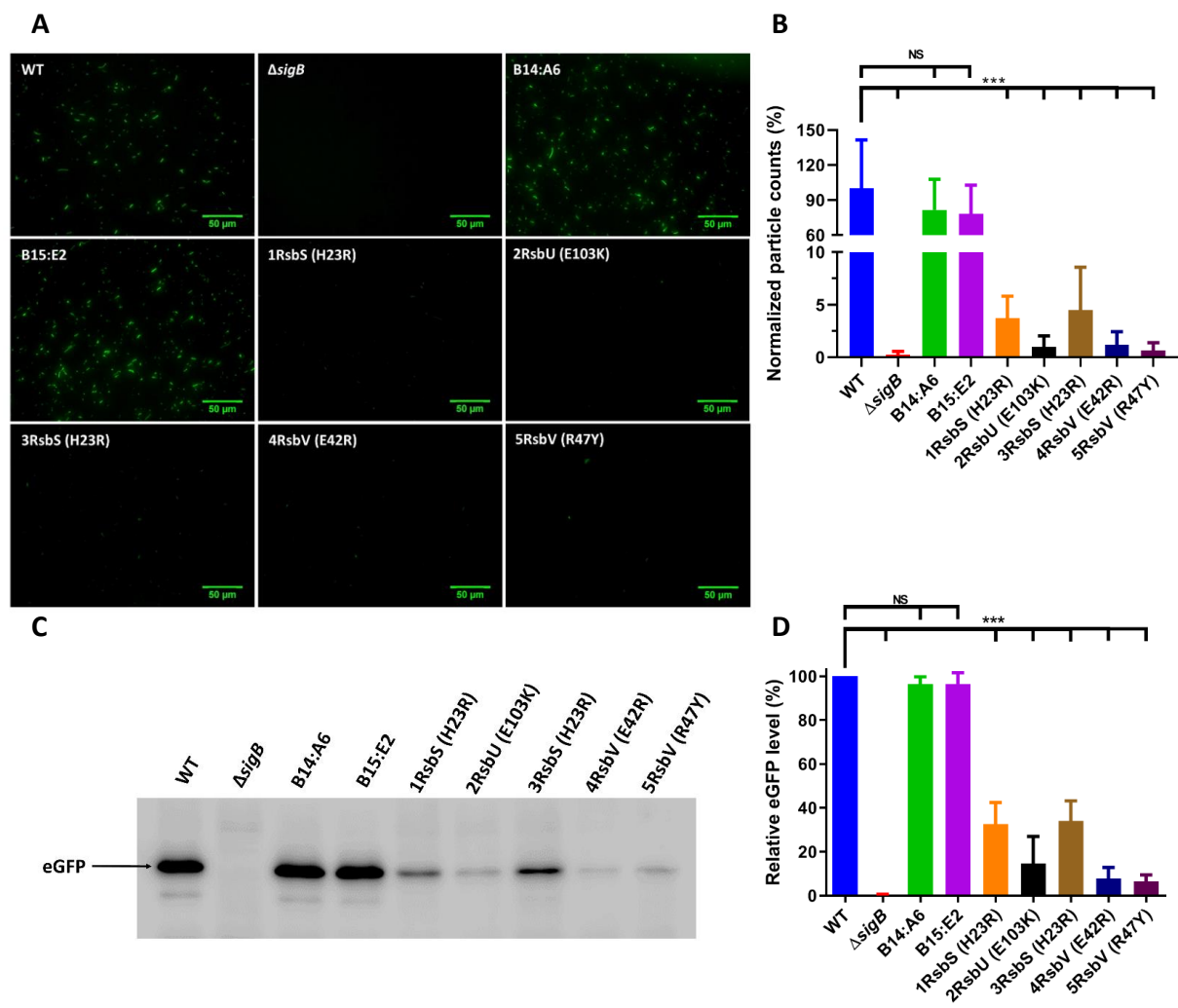


FIG 3 Transposon mutant strains carrying *sigB* operon mutations all have decreased σ^B activity. Stationary phase cultures grown at 37°C of WT, $\Delta sigB$ and transposon mutant strains transformed with pKSV7-P_{Imo2230}::*egfp*. Measurements of fluorescence were made through (A) images obtained by fluorescence microscopy (B) Particle quantification from fluorescence microscopy images. A total of 15 images were taken across three biological replicates. Particle counts were normalized against the WT strain and converted to percentage. (C) western-blot using anti-GFP antibodies, arrow shows eGFP protein with a size of 27 kDa. (D) Percentage of eGFP quantification normalized against the WT obtained from western-blot images. Data generated from three independent biological replicates. Statistical analysis performed through a paired Student *t*-test (* = *p*-value < 0.05; ** = *p*-value < 0.01; *** = *p*-value < 0.001; NS – non-significant).

1001

1002

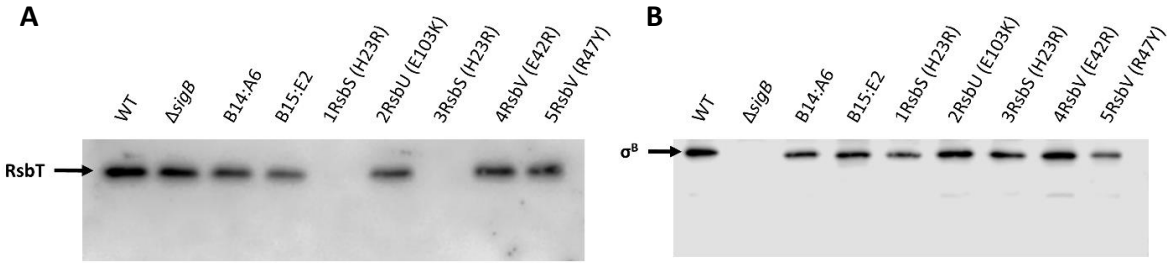


FIG 4 Frameshift mutations in *rsbS* produce a polar effect resulting in the inhibition of RsbT translation. Western-blot images obtained from total protein extractions of stationary phase WT, $\Delta sigB$, and transposon mutant strains grown at 37°C. Western-blot images were probed with rabbit polyclonal (A) anti-RsbT and (B) anti- σ^B antibodies. Arrows point to the respective proteins, RsbT with a predicted size of 14.7 kDa and σ^B with 29.5 kDa.

1003

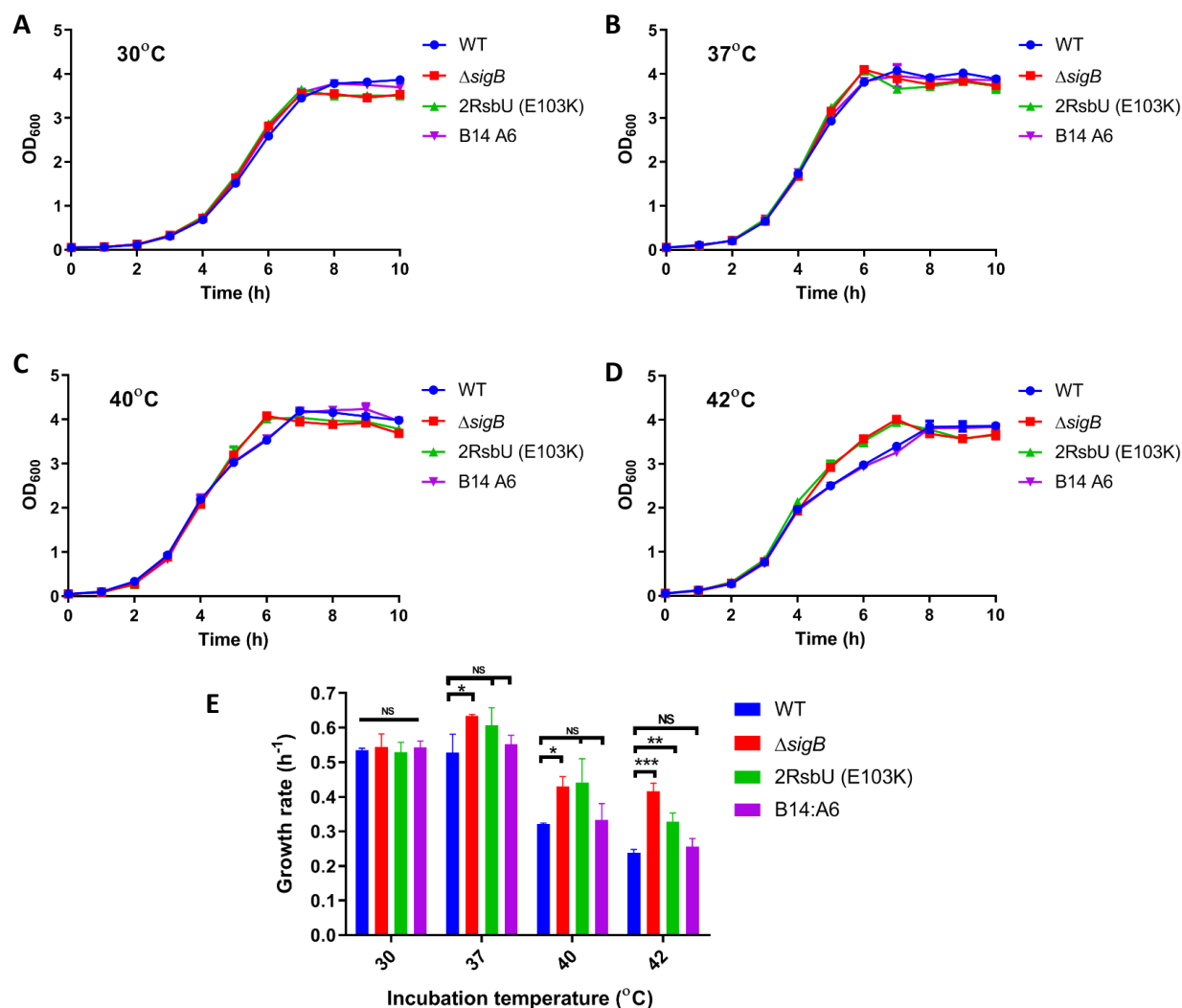


FIG 5 Loss of σ^B activity associated with increased growth rate at elevated temperatures. Measurements of OD₆₀₀ of WT, $\Delta sigB$, 2RsbU (E103K) and B14:A6 were performed every hour for 12 hours in BHI at (A) 30°C, (B) 37°C, (C) 40°C and (D) 42°C. (E) Growth rates in hours were calculated by using Log₁₀ (OD₆₀₀) of the transition period from data points between 4 and 5 hours (for 37°C, 40°C and 42°C) and 5 and 6 (30°C). Data generated for three biological replicates. Statistical analysis was performed using a paired Student *t*-test (* = *p*-value < 0.05; ** = *p*-value < 0.01; *** = *p*-value < 0.001; NS – non-significant).

1004

1005

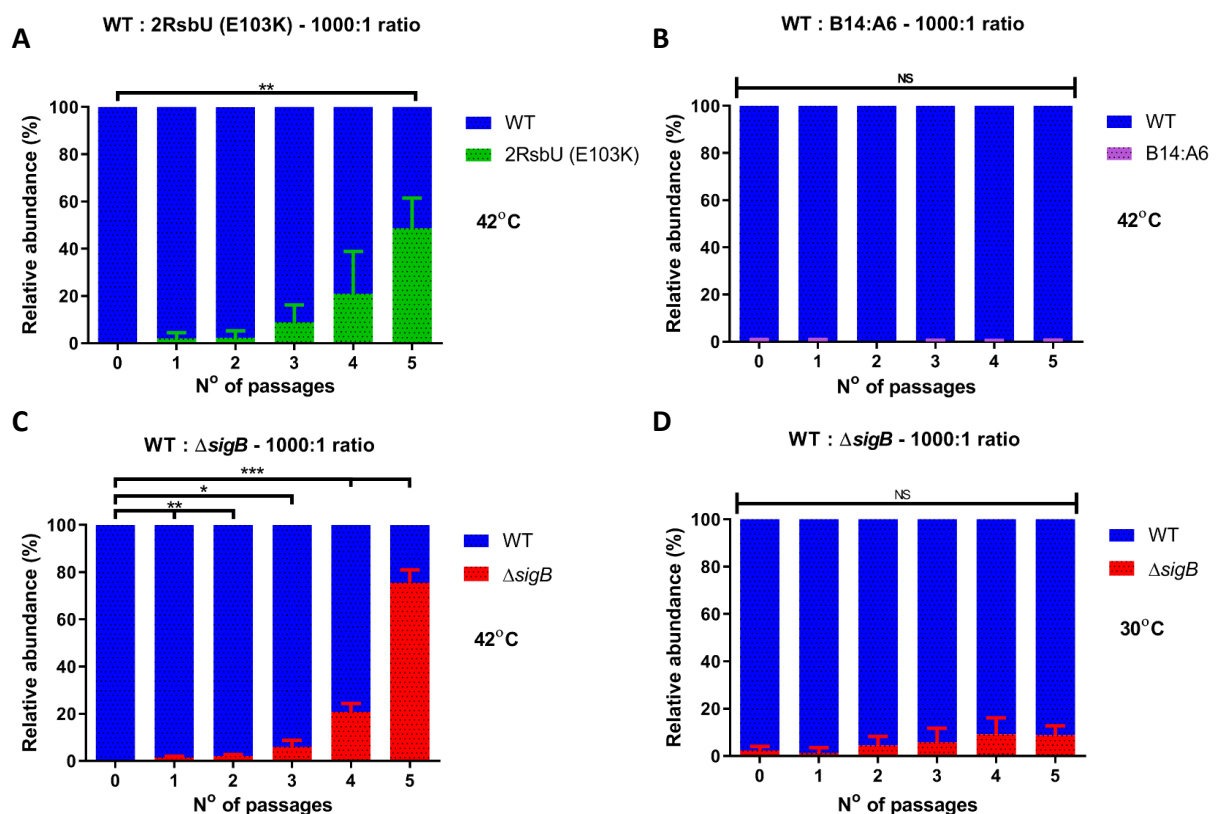


FIG 6 Loss of σ^B activity is associated with a competitive advantage at 42°C. Cultures mixed in ratios of 1000:1 of (A) WT with 2RsbU (E103K), (B) WT with B14:A6, (C) WT with $\Delta sigB$ incubated at 42°C and (D) WT with $\Delta sigB$ incubated at 30°C. Passages were made every 24 hours for 5 days. WT and transposon mutant strains were distinguished by erythromycin resistance. WT and $\Delta sigB$ mutant strains were distinguished by colony coloration. Results are depicted in relative abundance of CFU.mL⁻¹. Data generated for three independent biological replicates. Statistical analysis was performed using a paired Student *t*-test (* = *p*-value < 0.05; ** = *p*-value < 0.01; *** = *p*-value < 0.001; NS – non-significant).

1006

1007

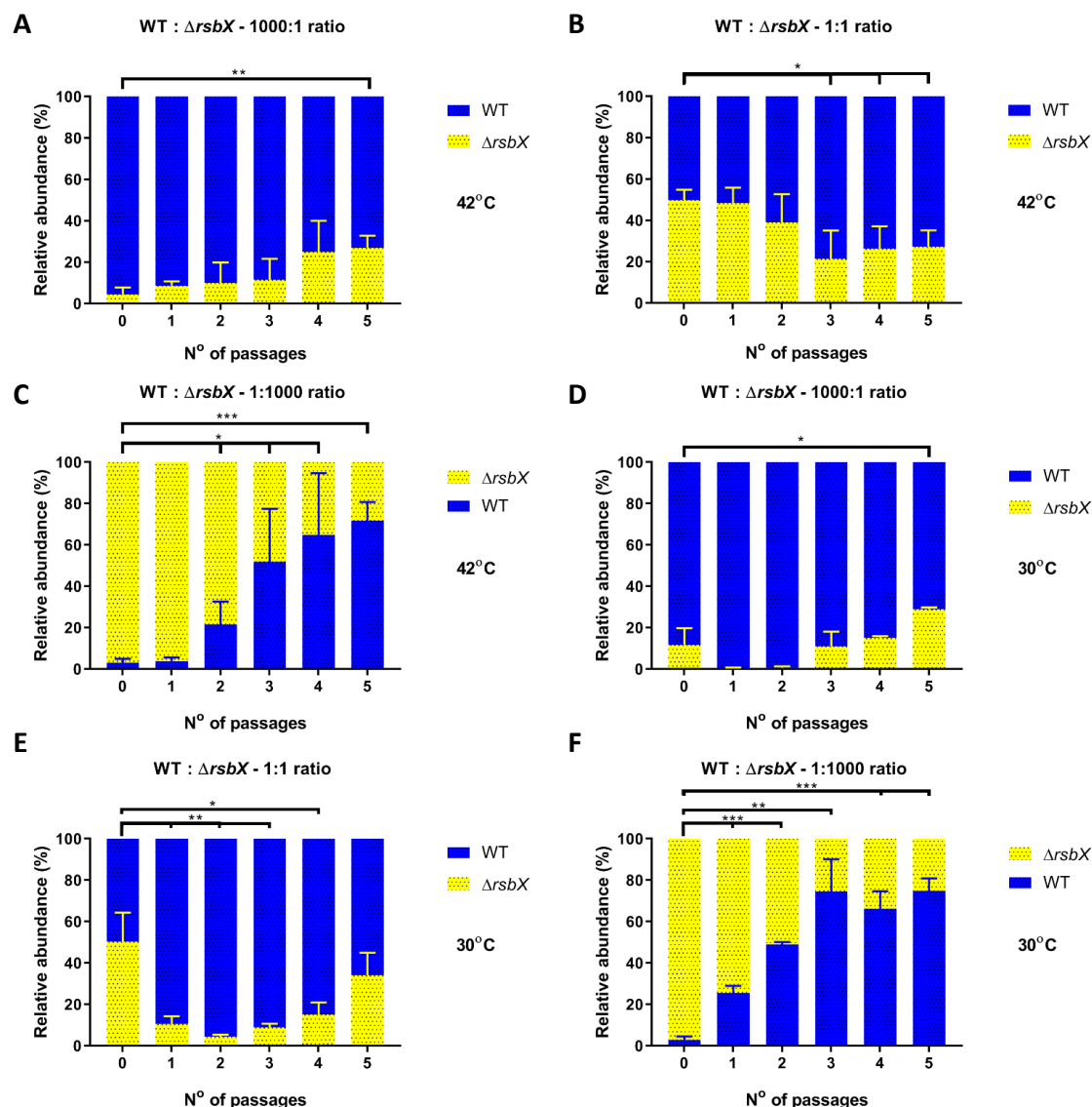


FIG 7 Competitive advantage of WT strain when challenged against $\Delta rsbX$ mutant strain at both 30°C and 42°C. Competition experiments of mixed cultures of WT and $\Delta rsbX$ mutant strains performed at 42°C and 30°C, showing the relative abundance in percentage of CFU.mL⁻¹. Cultures incubated at 42°C were mixed in ratios of (A) 1000:1 (B) 1:1, (C) 1:1000 of WT: $\Delta rsbX$, respectively. The same ratios were mixed and incubated at 30°C in (D), (E) and (F). Passages were made every 24 hours for 5 days. Statistical analysis performed through a paired Student *t*-test (* = *p*-value < 0.05; ** = *p*-value < 0.01; *** = *p*-value < 0.001).

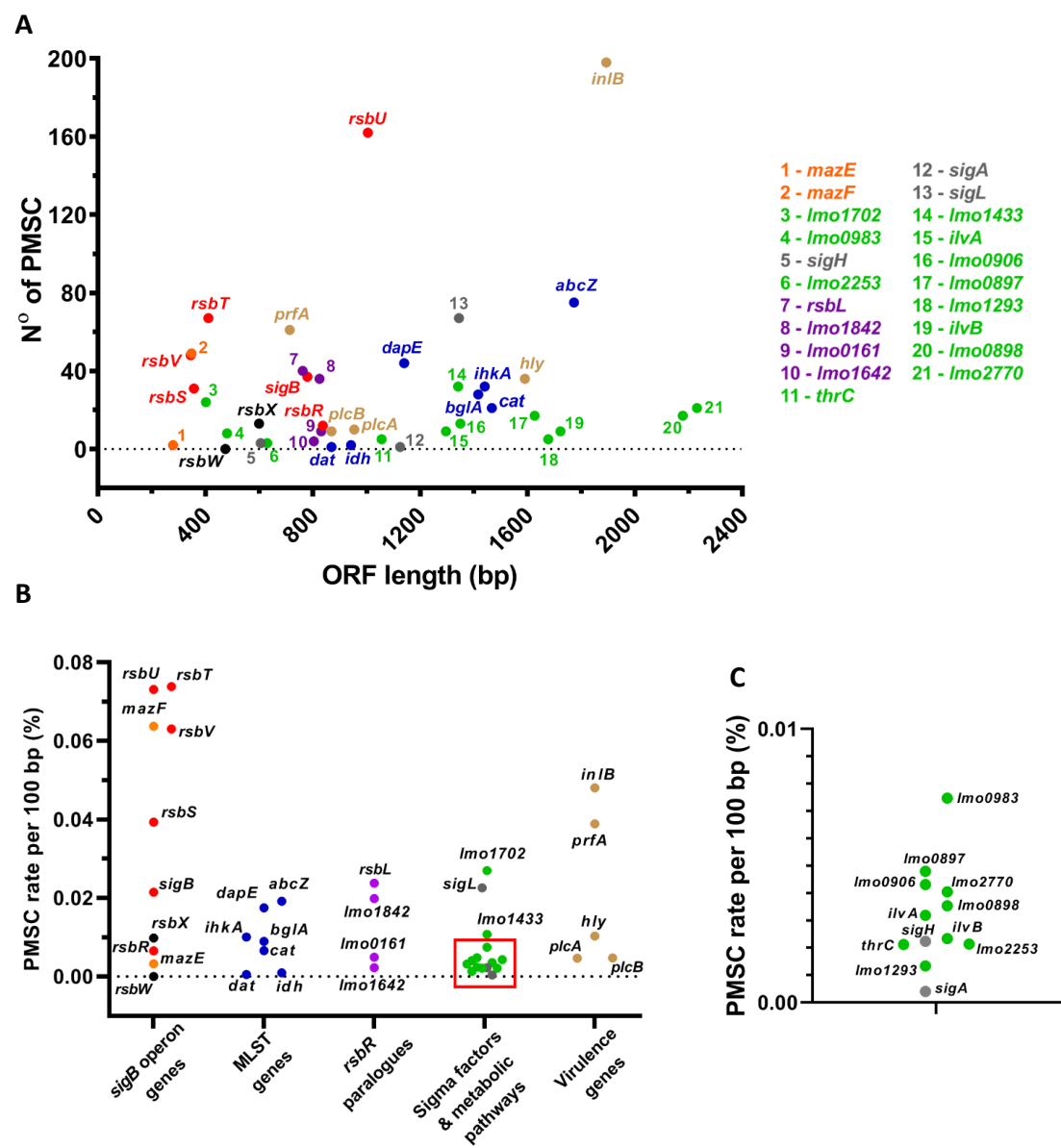


FIG 8 Occurrence of PMSCs is elevated in genes encoding positive effectors of σ^B activity. Results of the PMSC mutations retrieved from the *in silico* analysis of the 22,340 genomes *L. monocytogenes* strains available. (A) The total number of identified PMSC by the ORF length in base pairs and (B) PMSC rate normalized by 100 bp of the ORF length, displaying genes comprising the *sigB* operon and characterized as putative positive regulator of σ^B activity are displayed (red), the putative σ^B negative regulator *rsbX* and *rsbW* (black) and *mazEF* (orange) genes. MLST genes are displayed (blue), *rsbR* paralogues (purple). Housekeeping gene *sigA* and the sigma factors *sigL* and *sigH* (grey). Two genes downstream of the *sigB* operon, *lmo0897* and *lmo0898* and genes encoding for metabolic pathways of glutathione (*lmo1702*, *lmo0983*, *lmo1433*, *lmo0906* and *lmo2770*), glycerol (*lmo1293*), threonine (*thrC*), isoleucine (*ilvA* and *ilvB*) and glucose (*lmo2253*) (green) and *prfA*, *inlB*, *hly*, *plcA* and *plcB* (brown), respectively. The area indicated by the Red square area is expanded in (C).

1009

1010

Table 1 List of strains and plasmids used for this study.

Strains and plasmids ^a	Transposon ^b	Ring formation ^e	Source
pKSV7-P _{Imo2230} :: <i>egfp</i>	NA	NA	(24)
pMAD	NA	NA	(56)
pMAD::Δ <i>sigB</i>	NA	NA	(68)
pMAD::Δ <i>rsbX</i>	NA	NA	This study
pEX-K168::Δ <i>Imo0596</i>	NA	NA	Eurofins genomic
pMAD::Δ <i>Imo0596</i>	NA	NA	This study
<i>Escherichia coli</i> One Shot™ TOP10	NA	NA	Invitrogen
<i>L. monocytogenes</i> EGD-e WT	-	+	K. Boor
<i>L. monocytogenes</i> EGD-e Δ <i>sigB</i>	-	-	This study
<i>L. monocytogenes</i> EGD-e Δ <i>rsbX</i>	-	NA	This study
<i>L. monocytogenes</i> EGD-e Δ <i>Imo0596</i>	-	+	This study
<i>L. monocytogenes</i> EGD-e Δ <i>sreB</i>	-	+	(37)
<i>L. monocytogenes</i> EGD-e A4:E8 ^c (1RsbS (H23R)) ^d	+	-	(32)
<i>L. monocytogenes</i> EGD-e A4:D7 ^c	+	-	(32)
<i>L. monocytogenes</i> EGD-e A1:D10 ^c	+	-	(32)
<i>L. monocytogenes</i> EGD-e A4:B1 ^c	+	-	(32)
<i>L. monocytogenes</i> EGD-e A3:G10 ^c	+	-	(32)
<i>L. monocytogenes</i> EGD-e C10:A8 ^c ; (2RsbU (E103K)) ^d	+	-	(32)
<i>L. monocytogenes</i> EGD-e C14:C12 ^c ; (3RsbS (H23R)) ^d	+	-	(32)
<i>L. monocytogenes</i> EGD-e C12:F3 ^c	+	-	(32)
<i>L. monocytogenes</i> EGD-e C9:C1 ^c	+	-	(32)
<i>L. monocytogenes</i> EGD-e D9:B6 ^c ; (4RsbV (E42R)) ^d	+	-	(32)
<i>L. monocytogenes</i> EGD-e D2:C10 ^c ; (5RsbV (R47Y)) ^d	+	-	(32)
<i>L. monocytogenes</i> EGD-e B14:A6 ^c	+	+	(32)
<i>L. monocytogenes</i> EGD-e B15:E2 ^c	+	+	(32)
eGFP reporter strains			Source
<i>L. monocytogenes</i> EGD-e WT/pKSV7-P _{Imo2230} :: <i>egfp</i>			(24)
<i>L. monocytogenes</i> EGD-e Δ <i>sigB</i> /pKSV7-P _{Imo2230} :: <i>egfp</i>			This study
<i>L. monocytogenes</i> EGD-e A4:E8/pKSV7-P _{Imo2230} :: <i>egfp</i>			This study
<i>L. monocytogenes</i> EGD-e C10:A8/pKSV7-P _{Imo2230} :: <i>egfp</i>			This study
<i>L. monocytogenes</i> EGD-e C14:C12/pKSV7-P _{Imo2230} :: <i>egfp</i>			This study
<i>L. monocytogenes</i> EGD-e D9:B6/pKSV7-P _{Imo2230} :: <i>egfp</i>			This study
<i>L. monocytogenes</i> EGD-e D2:C10/pKSV7-P _{Imo2230} :: <i>egfp</i>			This study
<i>L. monocytogenes</i> EGD-e B14:A6/pKSV7-P _{Imo2230} :: <i>egfp</i>			This study

^a see Table 2 for full genotype description.^b presence/absence of chromosomal *mariner*-based transposon insertion.^c nomenclature consistent with Tiensuu et al. (32).^d transposon mutant strain new designation.^e Ring formation on soft agar plates in response to cycles of light/dark (ring formation requires σ^B)

NA – not applicable

1011

1012

1013 **Table 2 WGS results for *L. monocytogenes* EGD-e transposon mutant strains.**

Strain code (32)	Transposon location (32)	Transposon location (by WGS)	SNP location in <i>sigB</i> operon ^a	Frameshift result ^f	New strain name
A4:E8	<i>Imo0040</i>	<i>Imo0770</i> ^c	IN(<i>rsbS</i>)67 (+GATC)	p.H23Rfs*16	1RsbS (H23R)
A4:D7	<i>Imo0101/Imo0102</i> ^b	^e	IN(<i>rsbS</i>)67 (+GATC)	p.H23Rfs*16	NA
A1:D10	<i>Imo0842</i>	^e	IN(<i>rsbS</i>)67 (+GATC)	p.H23Rfs*16	NA
A4:B1	<i>Imo2682</i>	^e	IN(<i>rsbS</i>)67 (+GATC)	p.H23Rfs*16	NA
A3:G10	<i>Imo2777</i>	^e	IN(<i>rsbS</i>)67 (+GATC)	p.H23Rfs*16	NA
C10:A8	<i>Imo0124</i>	<i>Imo0125</i> ^c	Δ (<i>rsbU</i>)306 (-G)	p.E103Kfs*7	2RsbU (E103K)
C14:C12	<i>Imo0595/Imo0596</i> ^b	^e	IN(<i>rsbS</i>)67 (+GATC)	p.H23Rfs*16	3RsbS (H23R)
C12:F3	<i>Imo0774</i>	^e	Δ (<i>rsbU</i>)506 (-AT)	p.Y170Rfs*28	NA
C9:C1	<i>Imo1736</i>	^e	Δ (<i>rsbS</i>)6 (-T)	p.D21Efs*6	NA
D9:B6	<i>Imo0101</i>	<i>Imo0101/Imo0102</i> ^{b,c,d}	IN(<i>rsbV</i>)136 (+TGTAC)	p.R47Yfs*6	4RsbV (E42R)
D2:C10	<i>Imo2668</i>	^e	IN(<i>rsbV</i>)120 (+A)	p.E42Rfs*17	5RsbV (R47Y)
B14:A6	^g	<i>Imo1671</i>	None	NA	NA
B15:E2	^g	<i>Imo2287</i>	None	NA	NA

^a SNP position in *L. monocytogenes* chromosome identified by WGS.^b Transposon insertion located in intergenic region.^c Different transposon position than initially reported.^d Not in the same position as A4:D7.^e Same position as reported (32).^f Nomenclature adapted from Human Genome Variations Society (79). For example, in "p.H23Rfs*16", p.H23R refers to the first encoded residue affected in the new protein, resulting in a histidine to arginine substitution at the codon 23, while fs*16 refers to the number of codons in the new reading frame that would be translated prior to encountering a stop codon.^g Not previously analysed through WGS (32).

NA – not applicable.

1014

1015 **Table 3 List primers used for this study.**

1016	Primer sequence (5' to 3')	Target
1017	GCCTTGTCGCCATCTTTG	<i>egfp-lmo2230-F</i> integration
	GGCCGTTTACATCTCCATC	<i>egfp-lmo2230-R</i> integration
	ATAACGGCACAAAGCTTCG	<i>sigB</i> -flank_F
	TTATGGCGTCAACAGTCG	<i>sigB</i> -flank_R
	GGAGTAAATGAACAAGGCAG	<i>rsbX</i> -flank_F
	CGCTAGTTTTAAAAGGTGTTATGG	<i>rsbX</i> -flank_R
	CGGTCGACGTAGAGTCCATCGCCCGAA	<i>rsbX</i> -A
	TTACTCCACTTCCTCATTCTGCAAC	<i>rsbX</i> -B
	AATGAGGAAGTGGAGTAACCATAACACC	<i>rsbX</i> -C
	CGAGATCTATCATTCCGGCAACAAGTAAATCTTGG	<i>rsbX</i> -D
	CTAGCTAATGTTACGTTACA	pMAD-U
	GCGAGAAGAATCATAATGGG	pMAD-L
	GAAAATAAATTCCGGTTGCTAAGGC	<i>lmo0596-A</i>
	AATCGAGTCGGATGGTTCTTGTT	<i>lmo0596-B</i>
	CCACTCCTCTTTGATATGATTTAT	<i>lmo0596</i> -flank_F
	GGCAGATGAATGCACTTATG	<i>lmo0596</i> -flank_R
	Primer sequence for RT-qPCR (5' to 3')	Target
	TGGGGAGCAAACAGGATTAG	16S_F
	TAAGGTTCTTCGCGTTGCTT	16S_R
	CATATTGGAAGTGCCATTGC	<i>lmo2230_F</i>
	CTGAAGTGGTGAATAAGACAAAC	<i>lmo2230_R</i>
	CCTAAACTTGGATTTCGACTTATCTT	<i>sreB_F</i>
	TTCTTATCACGAAAGGTGGAGGG	<i>sreB_R</i>
	GGGTACTAGCTGACGGAATTTTATC	<i>lmo0596_F</i>
	CCCACATACCGAAAAGTAATACGAG	<i>lmo0596_R</i>